The Plant Cell, Vol. 27: 243–261, January 2015, www.plantcell.org

Recruitment of PLANT U-BOX13 and the PI4Kβ1/β2 Phosphatidylinositol-4 Kinases by the Small GTPase RabA4B Plays Important Roles during Salicylic Acid-Mediated Plant Defense Signaling in Arabidopsis[OPEN]

Vincenzo Antignani,[1] Amy L. Klocko,[1] Gwangbae Bak, Suma D. Chandrasekaran, Taylor Dunivin, and Erik Nielsen[2]

Department of Molecular, Cellular, and Developmental Biology, University of Michigan, Ann Arbor, Michigan 48109

Protection against microbial pathogens involves the activation of cellular immune responses in eukaryotes, and this cellular immunity likely involves changes in subcellular membrane trafficking. In eukaryotes, members of the Rab GTPase family of small monomeric regulatory GTPases play prominent roles in the regulation of membrane trafficking. We previously showed that RabA4B is recruited to vesicles that emerge from trans-Golgi network (TGN) compartments and regulates polarized membrane trafficking in plant cells. As part of this regulation, RabA4B recruits the closely related phosphatidylinositol 4-kinase (PI4K) PI4Kβ1 and PI4Kβ2 lipid kinases. Here, we identify a second *Arabidopsis thaliana* RabA4B-interacting protein, PLANT U-BOX13 (PUB13), which has recently been identified to play important roles in salicylic acid (SA)-mediated defense signaling. We show that PUB13 interacts with RabA4B through N-terminal domains and with phosphatidylinositol 4-phosphate (PI-4P) through a C-terminal armadillo domain. Furthermore, we demonstrate that a functional fluorescent PUB13 fusion protein (YFP-PUB13) localizes to TGN and Golgi compartments and that PUB13, PI4Kβ1, and PI4Kβ2 are negative regulators of SA-mediated induction of pathogenesis-related gene expression. Taken together, these results highlight a role for RabA4B and PI-4P in SA-dependent defense responses.

INTRODUCTION

Plants have a complex and sophisticated defense strategy to protect themselves from pathogenic organisms, which includes premade physical barriers as well as the accumulation of newly synthesized defense compounds. The perception of microbial pathogens occurs initially through the interaction of plasma-membrane localized receptor proteins of the host cell with pathogen-associated molecular pattern components (Liew et al., 2005). The detection of pathogen-associated molecular pattern components by these surface-localized receptors initiates defense signaling pathways that result in cellular responses to limit microbial growth and the induction of host disease resistance (Liew et al., 2005). One key feature of this system is a need for the trafficking and secretion of various molecules, including the secretion of antimicrobial proteins (van Loon et al., 2006) and reinforcement of the plant cell wall with callose, as first discovered in 1863 by de Bary (Nishimura et al., 2003). These trafficking processes must be carefully regulated to ensure that an effective defense response is achieved.

The Rab family of GTPase proteins are important regulators of membrane trafficking and cycle between an active GTP-bound form and an inactive GDP-bound form (Stenmark et al., 1994). In their active, GTP-bound forms, Rab GTPases recruit Rab effector proteins, and it is through these protein-protein interactions that they carry out their regulatory functions (Pereira-Leal and Seabra, 2001; Zerial and McBride, 2001; Vernoud et al., 2003). We previously showed that one member of the *Arabidopsis thaliana* RabA family, RabA4B, localizes to vesicles that emerge from the trans-Golgi network (TGN) and that this Rab GTPase plays important roles during the regulation of polarized membrane trafficking in root hair cells (Preuss et al., 2004; Kang et al., 2011). RabA4B specifically interacts with the lipid kinase isoforms phosphatidylinositol 4-kinase β1 (PI4Kβ1) and PI4Kβ2, and these proteins coordinate to regulate polarized expansion in root hairs (Preuss et al., 2006). However, RabA4B is widely expressed in numerous plant organs, including leaves (Preuss et al., 2004), and likely has additional functions outside of polarized cell growth. Rab GTPases also have been shown to interact with multiple effector proteins, and these effectors are diverse in both form and function (Grosshans et al., 2006).

To identify additional potential RabA4B effector proteins, a yeast two-hybrid (Y2H) screen for novel RabA4B effectors identified PUB13, a member of the Plant U-Box (PUB) family of E3 ligase proteins (Mudgil et al., 2004). While most PUB family members have not been extensively characterized, current evidence indicates that PUB proteins function in plant responses to various external cues. Arabidopsis PUB44 is required for delaying premature leaf senescence (Raab et al., 2009), while another Arabidopsis PUB family member, CHIP, is important for sensitivity to temperature stress (Yan et al., 2003). The oilseed rape (*Brassica napus*) ARM REPEAT CONTAINING1 (ARC1) is a positive regulator of self-incompatibility. ARC1 has verified E3

[1] These authors contributed equally to this work.

[2] Address correspondence to nielsene@umich.edu.

The author responsible for distribution of materials integral to the findings presented in this article in accordance with the policy described in the Instructions for Authors (www.plantcell.org) is: Erik Nielsen (nielsene@umich.edu).

[OPEN] Articles can be viewed online without a subscription.

www.plantcell.org/cgi/doi/10.1105/tpc.114.134262

ligase activity and is proposed to degrade stigmatic factors that are important for early events in pollen germination, thus leading to the rejection of self-pollen (Stone et al., 2003). S-receptor kinase is a known interacting partner that mediates the self-incompatibility response in oilseed rape. S-receptor kinase has been shown to interact and phosphorylate ARC1, which, in turn, acts as a positive regulator of the self-incompatibility response (Samuel et al., 2008). Loss of *Spl11*, a PUB homolog in rice (*Oryza sativa*), regulates flowering via interaction with SPL11-INTERACTING PROTEIN1, a Signal Transduction and Activation of RNA family member (Vega-Sánchez et al., 2008).

The closest Arabidopsis homolog to oilseed rape ARC1 is PUB17 (Yang et al., 2006). Unlike oilseed rape, Arabidopsis is self-compatible, and the function of PUB17 is unrelated to pollen-stigma interactions. Instead, PUB17 is important for the regulation of cell death during pathogen infection. Loss of PUB17 causes decreased resistance to the plant pathogen *Pseudomonas syringae* pv *tomato* DC3000 (*Pst* DC3000; Yang et al., 2006). Therefore, PUB17 is predicted to activate plant defense responses. Other PUB family members, PUB22, PUB23, and PUB24, function to downregulate defense responses (Trujillo et al., 2008). Similarly, loss of *Spl11* causes spontaneous lesion formation in the absence of infection and increased resistance to pathogens (Zeng et al., 2004). The increased resistance observed in these PUB mutants is thought to be due to the constitutive activation of defense responses, and Spl11 is proposed to be a negative regulator of cell death and defense. PUB13 was also recently shown to be involved in the regulation of salicylic acid (SA)-mediated resistance via the targeted degradation of the receptor protein FLAGELLIN SENSITIVE2 (FLS2) upon elicitation with flagellin (Lu et al., 2011; Li et al., 2012a, 2012b; Liu et al., 2012). These data show the importance of PUB proteins for responding to diverse extracellular signals in plants.

Here, we present data describing a functional connection between PUB13, RabA4B, and two other RabA4B-recruited effector proteins, PI4Kβ1 and PI4Kβ2, during SA-mediated defense responses to the pathogen *Pst* DC3000. We show by Y2H analysis that PUB13 specifically associates with RabA4B in a GTP-dependent manner through N-terminal U-box N-terminal domain (UND) and U-box domains. In vivo, a functional fluorescent fusion of PUB13 primarily localizes to internal subcellular compartments, and these EYFP-PUB13-labeled membranes display significant colocalization with the Golgi-localized syntaxin 32 marker protein ECFP-SYP32 (Geldner et al., 2009) and ECFP-RabA4B on Golgi-associated TGN compartments. Consistent with previous observations (Lu et al., 2011; Li et al., 2012a), *pub13* mutants were significantly smaller than wild-type plants and displayed an increased resistance to *Pst* DC3000. We describe similar reduced stature and increased pathogen resistance in *pi4kβ1/pi4kβ2* double mutant plants, and both mutant *pub13* and *pi4kβ1/pi4kβ2* double mutant plants display constitutively induced expression of SA-dependent *PATHOGENESIS RELATED* (*PR*) genes and increased levels of ectopic deposition of callose in leaves. We also demonstrate that PUB13 interacts directly with phosphoinositides, including phosphatidylinositol 4-phosphate (PI-4P), through C-terminal sequences. We propose that RabA4B orchestrates the regulation of SA-mediated defense response by recruiting and trafficking of the effectors PUB13, PI4Kβ1, and PI4Kβ2, which normally function to suppress the induction of SA-mediated defense responses in uninfected plants.

RESULTS

PUB13 Is a RabA4B-Interacting Protein

In order to identify additional RabA4B effector proteins, we used a Y2H screen to find proteins that interact with constitutively active (GTP-bound) RabA4B. Out of 127 sequenced yeast colonies containing putative RabA4B-interacting proteins, we identified one clone that contained the N-terminal region of PUB13 (amino acids 1 to 551, termed PUB13 Δ552-660). Rab GTPases interact with their effector proteins in a manner regulated by GTP binding and hydrolysis, with Rab effector protein interactions being stabilized when the Rab GTPase is in a GTP-bound state and this interaction being lost upon hydrolysis of GTP to GDP (Hutagalung and Novick, 2011). To determine if the interaction between PUB13 and RabA4B was nucleotide-dependent and specific to RabA4B, we also tested the interaction of PUB13 with RabG3C, RabF2A, and the small GTPase ROP1, which localize to plant vacuolar, endosomal, and plasma membrane compartments, respectively (Ueda et al., 2001; Gu et al., 2005; Haas et al., 2007). We found that PUB13 interacts with the active, GTP-bound form of RabA4B but not with a GDP-locked mutant form (Figure 1A). Additionally, PUB13 did not interact with other members of the Rab family or with ROP1 (Figure 1A). From these data, we concluded that PUB13 is a potential effector of RabA4B.

We were interested to determine which domains of PUB13 are responsible for interaction with RabA4B. PUB13 contains three domains, the UND (amino acids 1 to 255), a U-box domain (amino acids 256 to 328), and a series of six armadillo (ARM) repeats (amino acids 383 to 587) (Figure 1B). We tested these domains singly and in combination and determined that the UND-U-box domain combination is necessary for interaction with active RabA4B (Figure 1C). We were unable to detect Y2H interaction between full-length PUB13 and RabA4B; however, this may be a reflection of the experimental method, as the full length of the RabA4B effector protein PI4Kβ1 also fails to interact with RabA4B in a Y2H assay, even though full-length PI4Kβ1 interacts with RabA4B in a biochemical assay (Preuss et al., 2006).

To determine whether PUB13 is capable of interacting directly with RabA4B, we performed a far-western protein gel blot experiment, where different dilutions of recombinant PUB13-UND-U-box protein were spotted onto a nitrocellulose membrane and then hybridized with RabA4B bound to a nonhydrolyzable form of GTP (RabA4B-GTPγS). Recruitment of RabA4B was detected with anti-RabA4B antibody (Figure 2A). To confirm the interaction between RabA4B and PUB13 in planta, we performed bimolecular fluorescence complementation (BiFC; Hu et al., 2002), where the constitutively active form of RabA4B was fused to the N-terminal portion of yellow fluorescent protein (YFP) (nYFP-RabA4B) or to the C-terminal portion of YFP (RabA4B-cYFP), while PUB13 was fused to the C-terminal portion of YFP (PUB13-cYFP) and to the N-terminal portion of YFP (nYFP-PUB13). Then, nYFP and cYFP fusions proteins were transiently expressed in *Nicotiana benthamiana* leaf epidermal cells. The relative level of reconstituted BiFC fluorescence was detected by confocal

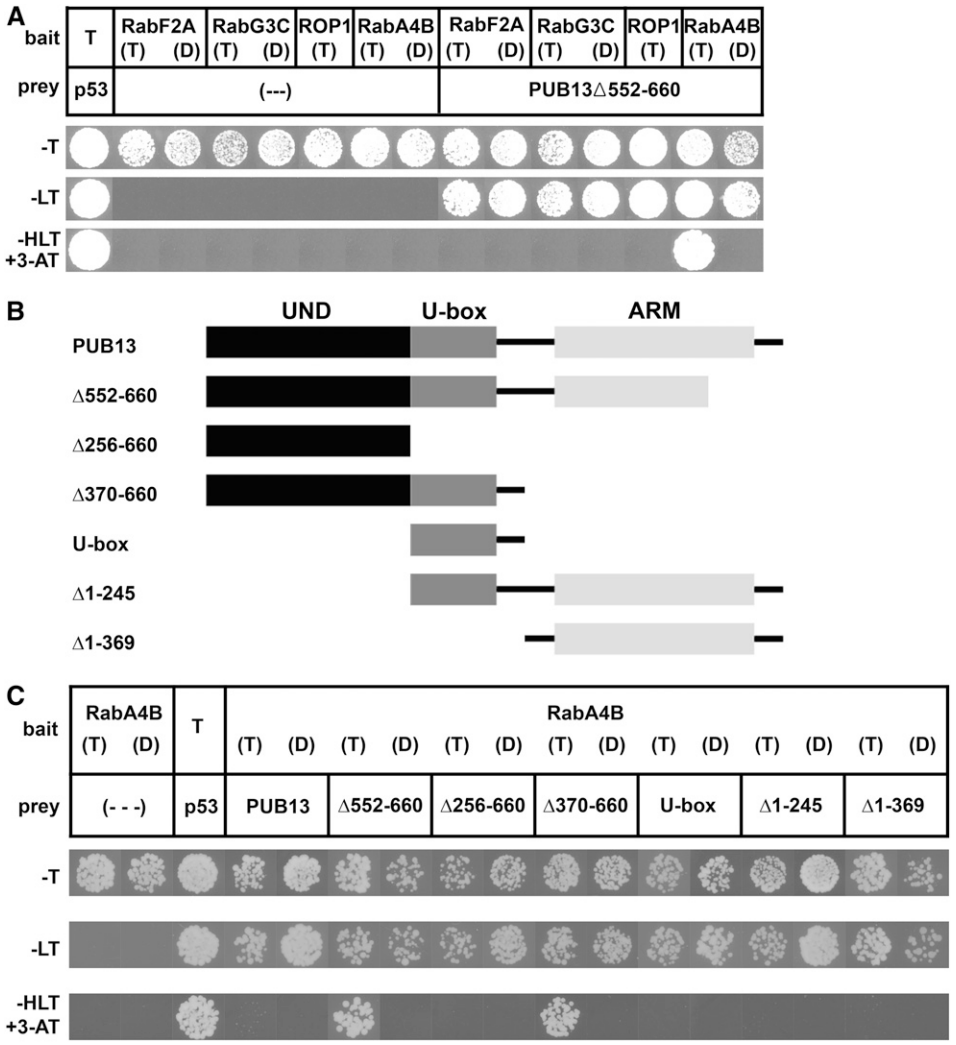

Figure 1. PUB13 Interacts Specifically with the Active Form of RabA4B.

(A) Y2H interaction of PUB13Δ552-660 with active GTP-bound RabA4B (T), but not inactive GDP-bound RabA4B (D), was detected on high-stringency medium (−HisTrpLeu + 3-aminotriazole [−HTL+3-AT]). No interaction was observed with RabF2A, RabG3C, and ROP1. The presence of prey and/or bait vectors was monitored by growth in the absence of leucine and tryptophan (−LT) or tryptophan (−T), respectively.

(B) UND, U-box, and ARM domains are indicated. Deletion fragments of PUB13 were constructed to determine the binding site of RabA4B.

(C) Y2H interaction was seen between active RabA4B and PUB13 fragments on selective medium (−HisTrpLeu+3-AT). The interaction between RabA4B and PUB13 requires the presence of UND and U-box domains. No interaction was observed between RabA4B and the ARM domain. Surprisingly, full-length PUB13 did not interact with RabA4B in the Y2H assay.

microscopy in leaves prestained with propidium iodide to detect cell peripheries (Figure 2B). While we did observe that minimal levels reconstituted BiFC fluorescence when nYFP alone was coexpressed with PUB13-cYFP (Figure 2B, panel 2) or when nYFP-RabA4b was coexpressed with cYFP alone (Figure 2B, panel 3), the level of reconstituted BiFC fluorescence was significantly enhanced when RabA4B and PUB13 were both present (Figure 2B, panels 1 and 4). Reconstituted BiFC fluorescence could not be detected in cells that expressed only nYFP-RabA4B or cYFP-PUB13 (Figure 2B, panels 5 and 6). To further characterize the levels of reconstituted BiFC fluorescence, fluorescence in leaves expressing these nYFP and cYFP constructs was quantified. The mean YFP fluorescence intensity of the epidermis increased to approximately five times the initial value in cells when both RabA4B and PUB13 were expressed (Figure 2C, black bars). These results, taken together with our Y2H (Figure 1) and in vitro far-western protein gel blot (Figure 2A) results, support the conclusion that PUB13 can interact physically with RabA4B, likely through interaction with the UND-U-box domains, both in vitro and in vivo.

PUB13 Localizes to Golgi and TGN Compartments

We examined whether RabA4b and PUB13 colocalized to the same subcellular membranes in Arabidopsis cells. To determine

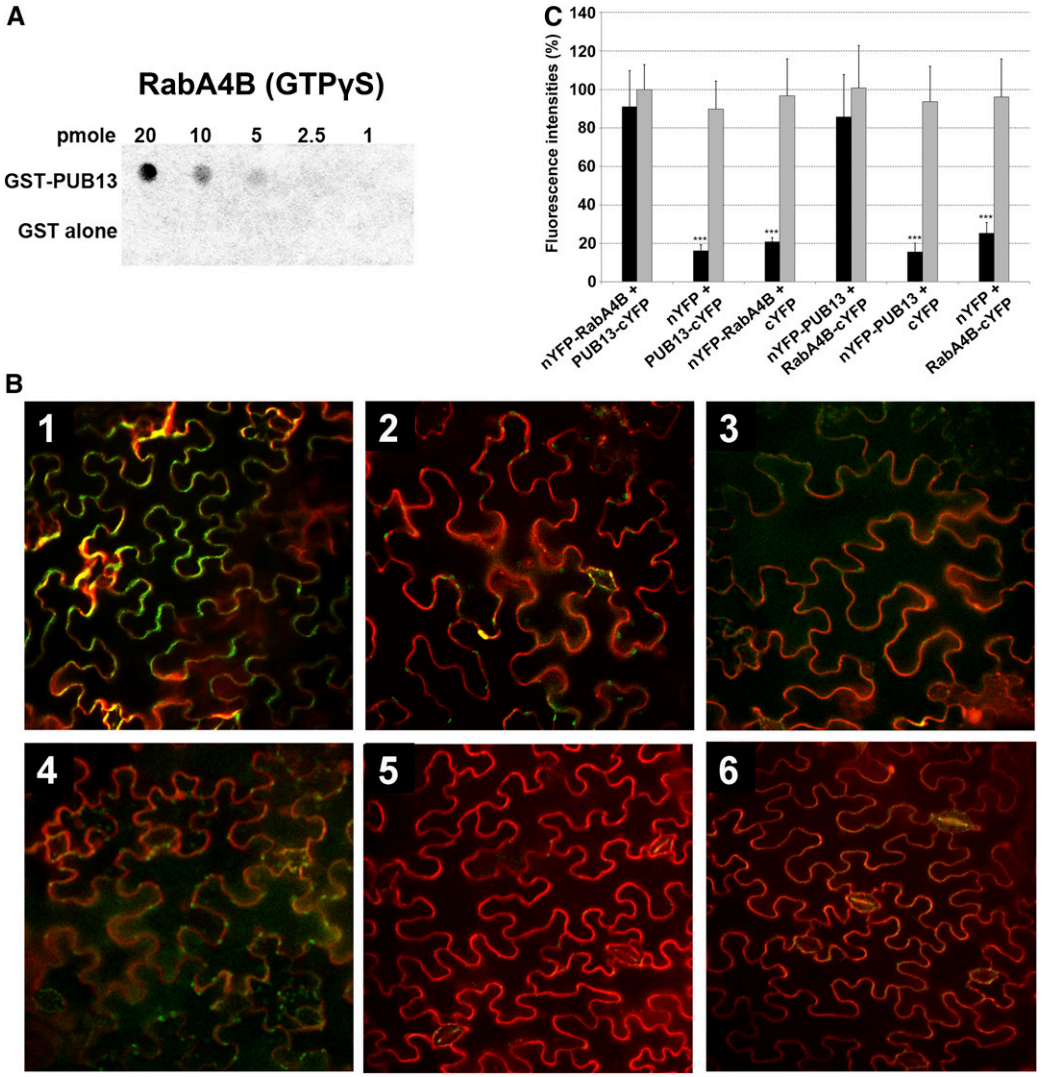

Figure 2. The Physical Interaction between PUB13 and RabA4B Was Confirmed in a Far Protein Gel Blot and BiFC.

(A) Different dilutions of recombinant PUB13 were spotted onto a nitrocellulose membrane and then hybridized with 25 nM RabA4B-GTPγS. RabA4B was recruited by PUB13, and the recruitment was detected using an anti-RabA4B antibody.

(B) BiFC assays using RabA4B and PUB13 to reconstruct the YFP signal. A strong interaction was detected in leaves expressing nYFP-RabA4B and PUB13-cYFP (panel 1). BiFC fluorescence intensity was weaker in leaves expressing nYFP-PUB13 and RabA4B-cYFP fusion domains (panel 4). No significant fluorescence was detected when only one of the fusion proteins was expressed with the complementary portion of YFP (panels 2, 3, 5, and 6). Panels are as follows: 1, nYFP-RabA4B with PUB13-cYFP; 2, nYFP with PUB13-cYFP; 3, nYFP-RabA4B with cYFP; 4, nYFP-PUB13 with RabA4B-cYFP; 5, nYFP-PUB13 with cYFP; 6, nYFP with RabA4B-cYFP. Leaves were treated with propidium iodide to stain the outline of the cell.

(C) BiFC (black bars) and propidium iodide (gray bars) fluorescence intensities were quantified as mean values of YFP and RFP fluorescence intensity, respectively (mean ± SD, $n = 50$). Asterisks indicate significant differences ($P < 0.001$) calculated by Student's t test.

the distribution of PUB13, we examined the subcellular localization of a functional EYFP-PUB13 fluorescent fusion protein that was stably transformed into Arabidopsis seedlings, which were then crossed with plants harboring either enhanced cyan fluorescent protein (ECFP)-conjugated RabA4B or the Golgi-localized red fluorescent protein (RFP)-SYP32 (Geldner et al., 2009). In these lines, the EYFP-PUB13 fusion protein selectively labeled mobile punctate structures (Supplemental Movie 1) in both leaf epidermal (Figures 3A to 3C) and root epidermal (Figures 3D to 3F) cells. While the YFP-PUB13-labeled structures displayed significant levels of colocalization (63.6%) with CFP-RabA4B in leaf tissues (Figure 3C), the degree of colocalization (29.14%) of these two fusion proteins in root tissues was significantly lower (Figure 3F). EYFP-PUB13 also displayed similar levels of colocalization with the RFP-SYP32-labeled Golgi compartments (63.41%) in leaf epidermal cells (Figures 3G to 3I). However, unlike ECFP-RabA4B, EYFP-PUB13 colocalization levels with the RFP-SYP32 marker were maintained (73.47%) in root tissues (Figures 3J to 3L). In growing root hairs, EYFP-PUB13 labeled mobile Golgi-like structures, but no significant accumulation was observed in the

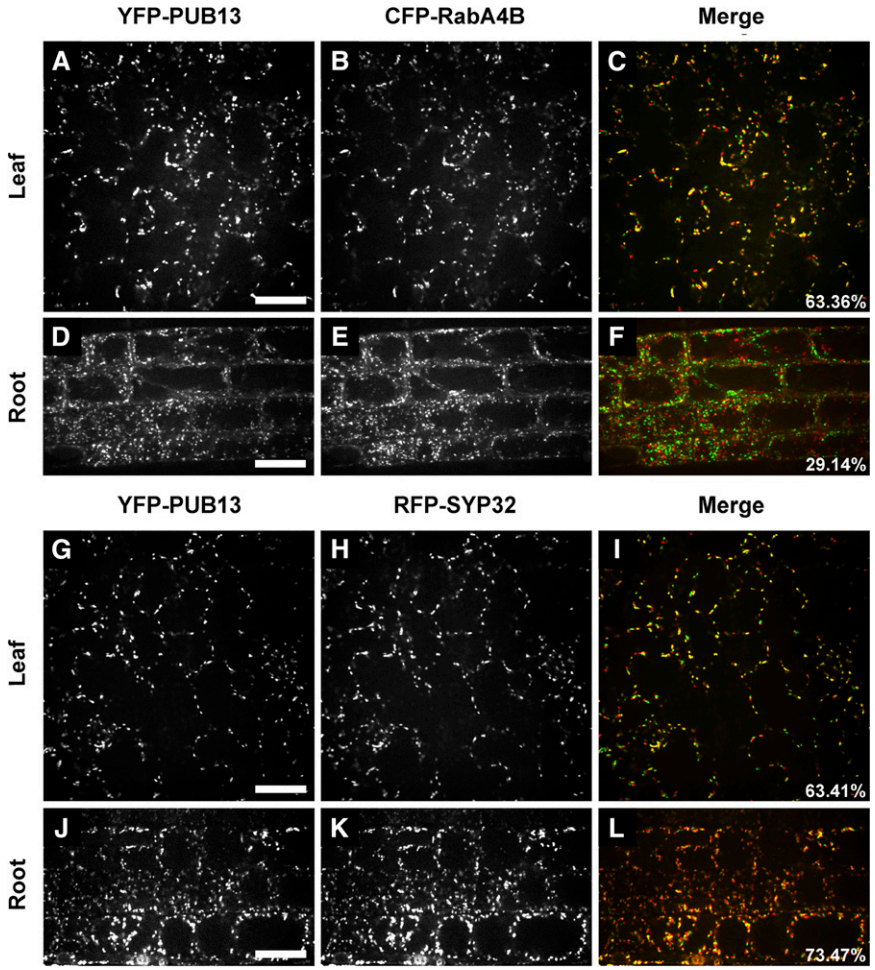

Figure 3. PUB13 Localizes on the TGN and Golgi.

Leaf tissues coexpressing YFP-fluorescent PUB13 (**[A]** and **[G]**) together with CFP-RabA4B **(B)** or together with RFP-SYP32 **(H)**, and merged images (**[C]** and **[I]**), are shown. Note the colocalization (yellow signal) on TGN and Golgi (the percentage of overlapping fluorescent signals). Root epidermal cells coexpressing YFP-PUB13 (**[D]** and **[J]**) together with CFP-RabA4B **(E)** or together with RFP-SYP32 **(K)**, and merged images (**[F]** and **[L]**), are shown. Note the colocalization (yellow signal) on TGN and Golgi (the percentage of overlapping fluorescent signals). Bars = 15 μm.

tips of these cells (Supplemental Movie 1). Taken together, these results indicate that EYFP-PUB13 labeled compartments that partially colocalize both with Golgi-localized RFP-SYP32 compartments and with a subset of CFP-RabA4B-labeled compartments. However, this colocalization is restricted to Golgi/TGN subcellular membranes and is not observed in TGN-derived RabA4B-labeled secretory vesicles in tip-growing root hair cells.

Mutant *pub13* and *pi4kβ1/pi4kβ2* Double Mutant Plants Display Similar Growth Defects

To gain a better understanding of PUB13 function during plant growth and development, we obtained a SALK T-DNA insertion line for *PUB13*. We performed RT-PCR analysis on wild-type Columbia-0 (Col-0) plants and homozygous *PUB13* mutant (*pub13*) plants. The *pub13* plants showed disrupted expression of *PUB13* transcript as compared with wild-type (Col-0) plants (Supplemental Figure 1A). We observed that plants homozygous for the T-DNA insertion in *PUB13* displayed defects in growth and development and were significantly smaller than wild-type plants (Figure 4A), confirming observations reported previously by Li et al. (2012a). Growth defects observed for *pub13* could be complemented by expressing EYFP-PUB13 fusion protein (Supplemental Figure 1B). Intriguingly, we noted that the aerial growth phenotypes, which we and others (Li et al., 2012a) described for the *pub13* mutant, were strikingly similar to those described previously for *pi4kβ1/pi4kβ2* double knockout mutants (Preuss et al., 2006), in which the expression of two other RabA4B effector proteins, PI4Kβ1 and PI4Kβ2, was eliminated. However, while both *pub13* and *pi4kβ1/pi4kβ2* plants displayed similar aerial growth defects (Figure 4A), *pi4kβ1/pi4kβ2* double mutants also displayed defects in tip-growing root hairs (Figures 4B and 4D), but root hairs of *pub13* mutant plants were normal (Figures 4B and 4C).

In order to determine whether the growth phenotypes observed for *pi4kβ1/pi4kβ2* double mutants were actually due to the loss of PI4K activity, we tested whether a catalytically inactive form of

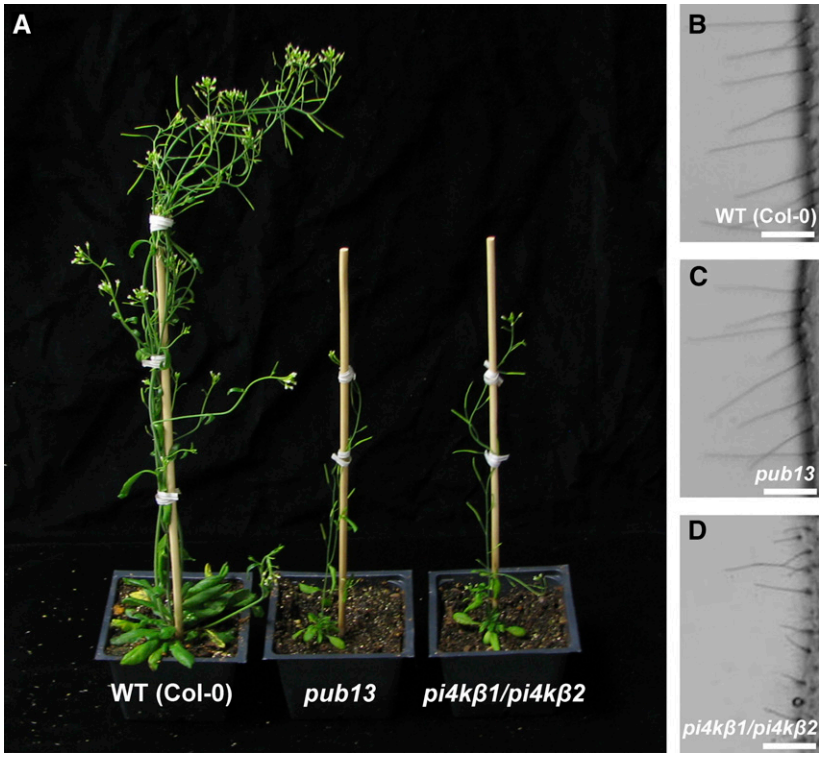

Figure 4. PUB13 Function Is Essential for Normal Aerial Growth in Arabidopsis but Not for Root Hair Development.

The *pub13* homozygous mutant plants were significantly smaller than wild-type (Col-0) plants **(A)**. Despite the close similarity of the aerial parts between *pub13* and *pi4kβ1/pi4kβ2* **(A)** mutants, *pub13* plants did not show impaired root hair development **(C)**. Panels are as follows: aerial part of wild-type (Col-0), *pub13* homozygous mutant, and *pi4kβ1/pi4kβ2* homozygous mutant plants **(A)**; wild-type (Col-0) root hairs **(B)**; *pub13* homozygous mutant root hairs **(C)**; and *pi4kβ1/pi4kβ2* homozygous mutant root hairs **(D)**. Bars = 200 μm.

PI4Kβ1 (*PI4Kβ1 D972A*; Strahl et al., 2005) was able to restore aerial and root hair growth phenotypes in *pi4kβ1/pi4kβ2* plants (Supplemental Figure 2). This mutation is based on an invariant residue present in the catalytic domain of all PI4Ks and is required for Pik1p activity in yeast (Strahl et al., 2005). We found that the expression of catalytically inactive PI4Kβ1 was unable to rescue either aerial (Supplemental Figure 2A) or root hair growth defects (Supplemental Figures 2B to 2D). Significantly, expression of the catalytically inactive PI4Kβ1 D972A mutant did not rescue the constitutively activated expression of the *PR1* gene in *pi4kβ1/pi4kβ2* plants (Supplemental Figure 2E). Furthermore, PI4Kβ1 and PI4Kβ2 interact with RabA4B through a novel-homology domain that is spatially distinct from the catalytic site, and these interactions occur independently of the presence of the catalytic domain (Preuss et al., 2006). These results suggest that these phenotypes are the result o loss of PI4Kβ1/2-associated PI4K activity and not simply due to a structural deficiency caused by the lack of accumulation of these proteins.

RabA4B Effector Mutants Display Enhanced Resistance to *Pst* DC3000

Previous characterization of *pub13* mutant plants showed that they had increased resistance to biotrophic and necrotrophic pathogens (Lu et al., 2011; Li et al., 2012a). Since similar growth defects were observed for *pi4kβ1/pi4kβ2* double mutants, we were interested in determining whether they also display increased pathogen resistance. Therefore, we compared how loss of either *PUB13* or *PI4Kβ1/β2* affected the ability of *Pst* DC3000 to grow and induce disease symptoms in these mutant plants. The rate of bacterial growth inside leaves was significantly lower for *pub13* and *pi4kβ1/pi4kβ2* compared with wild-type plants (Figure 5; $n = 30$). In both *pub13* and *pi4kβ1/pi4kβ2* plants, scoring of disease symptoms was similar, with a limited percentage of plants (50%) showing clear symptoms of bacterial disease, while over 95% of the wild-type plants manifested serious signs of bacterial infection. Disease signs were scored based on the emergence of water-soaked areas (starting from 3 d after inoculation), which then developed into necrosis, chlorosis, and, in the most extreme case, wilting of the whole plant. Purpling of the leaf tissues (possibly due to the accumulation of anthocyanins) was sporadically observed. These results indicate that *PUB13* and the two lipid kinases, *PI4Kβ1* and *PI4Kβ2*, both play important roles during the initiation and establishment of defense responses to *Pst* DC3000.

RabA4B-Interacting Protein Mutants Display Callose Deposition in the Absence of Pathogens

One physiological outcome of pathogen-related signaling is the induction of ectopic callose deposition in the cell walls of infected

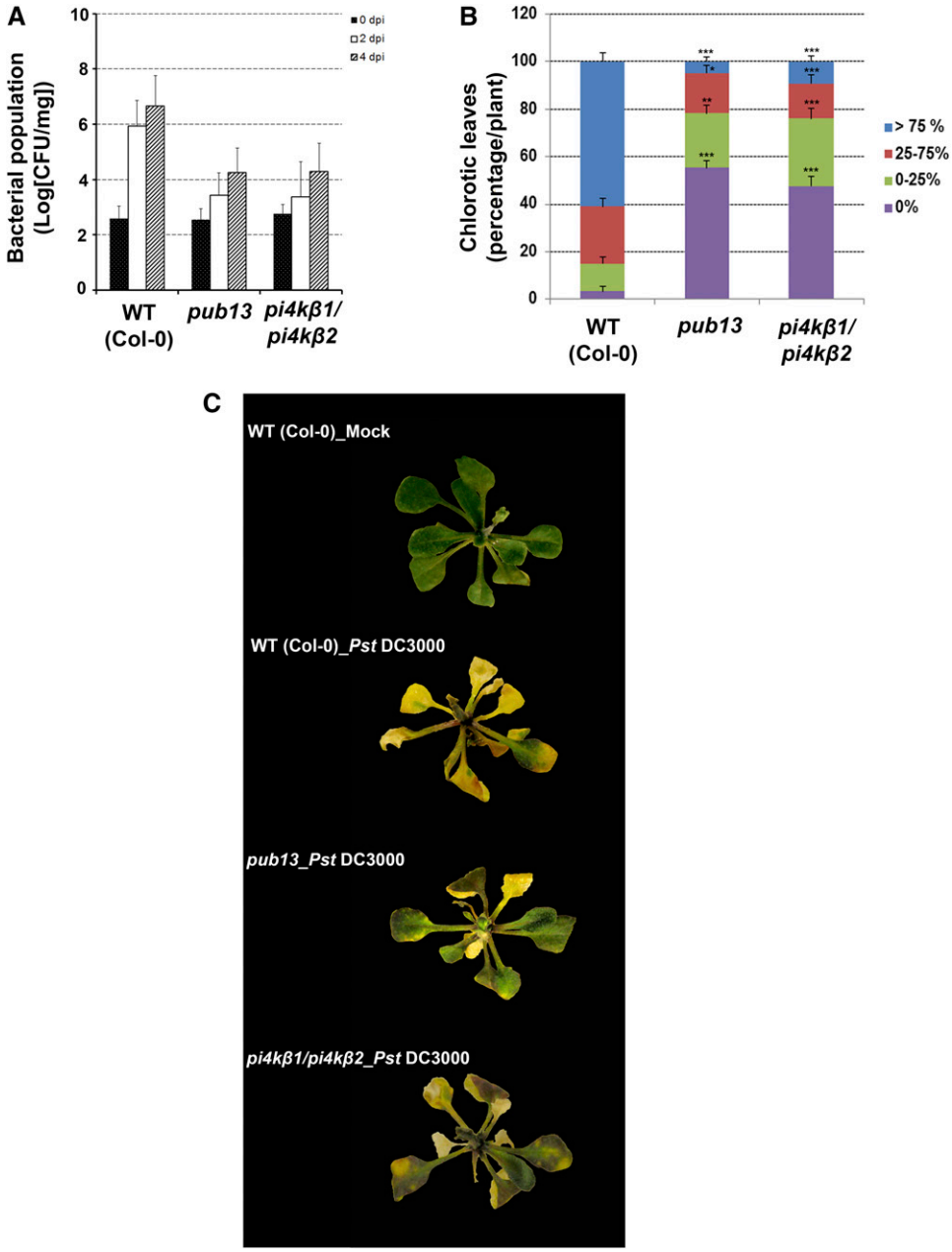

Figure 5. *pub13* and *pi4kβ1/pi4kβ2* Mutant Plants Display Enhanced Resistance to *Pst* DC3000.

Wild-type (Col-0), *pub13*, and *pi4kβ1/pi4kβ2* plants were flood-inoculated with a suspension of bacterial cells (1×10^5 colony-forming units [CFU]).
(A) Bacterial growth on leaf tissue.
(B) and **(C)** Chlorotic symptoms in plants 4 d after inoculation. The data shown are means ± SD from 30 leaves, with three replicates for each genotype. Asterisks indicate significant differences at $P < 0.1$ (*), $P < 0.05$ (**), and $P < 0.01$ (***) between wild-type (Col-0) and *pub13* plants or between wild-type (Col-0) and *pi4kβ1/pi4kβ2* plants. P values were calculated by Student's *t* test.

plants (DebRoy et al., 2004). To assess the presence of ectopic callose deposition in *pub13* and *pi4kβ1/pi4β2* mutant plants, we collected rosette leaves from uninfected 4-week-old plants and stained for callose using decolorized aniline blue (Figure 6). Leaves from both *pub13* and *pi4kβ1/pi4kβ2*, but not wild-type plants, displayed numerous fluorescent patches indicating an enhanced deposition of callose in these tissues (Figures 6A to 6C and 6G).

In Arabidopsis, the perception of the bacterial component flagellin by the membrane receptor FLAGELLIN-SENSITIVE2 (FLS2) leads to the deposition of callose in the cell wall (Bardoel et al., 2011; Lu et al., 2011), and we wondered whether PUB13, PI4Kβ1, and PI4Kβ2 are also involved in the signaling of callose deposition. To test this hypothesis, we stimulated leaves of wild-type, *pub13*, and *pi4kβ1/pi4kβ2* plants with flagellin fragment 22

(flg22), which revealed little difference among the three genotypes (Figures 6D to 6F and 6G), suggesting that *pub13* and *pi4kβ1/pi4kβ2* mutant plants have normal responses to flagellin and a functional FLS2 receptor and signaling pathway.

Mutation of RabA4B-Interacting Proteins Constitutively Activates SA-Dependent *PR* Gene Expression

One possible explanation for the decreased growth rate, increased resistance, and increased callose deposition observed in *pub13* and *pi4kβ1/pi4kβ2* double mutant plants when exposed to pathogens is the constitutive activation of plant defenses in the absence of pathogens (Bowling et al., 1994). Expression of *PR* genes is an early occurrence in plant defenses (van Loon et al., 1994; van Loon and van Strien, 1999). We compared the relative expression levels of *PR* genes (*PR1* to *PR5*) in *pub13*, *pi4kβ1/pi4kβ2*, and wild-type plants in the absence of pathogen challenge. Using RT-PCR, we found that *PR1*, *PR2*, and *PR5* expression levels were higher in 4-week-old *pub13* and *pi4kβ1/pi4kβ2* plants compared with wild-type plants (Figure 7A). These results were confirmed by using quantitative RT-PCR (qRT-PCR), and we concluded that *PR1*, *PR2*, and *PR5* expression levels were increased between 30- and 50-fold in *pub13* and *pi4kβ1/pi4kβ2* plants, whereas the expression of *PR3* and *PR4* was either unchanged or only slightly induced (Figure 7B). Expression of *PR1*, *PR2*, and *PR5* has been shown to be regulated by the plant hormone SA (Uknes et al., 1992).

We inferred that it is likely that in *pub13* and *pi4kβ1/pi4kβ2* plants, SA-mediated defense genes are constitutively expressed even in the absence of pathogen challenge. In the case of *pub13* mutant plants, constitutive activation of *PR1* gene expression was specific to the loss of *PUB13* activity and normal *PR1* gene expression was restored in stably transformed *pub13* expressing either *EYFP-PUB13* or untagged *PUB13* genes (Supplemental Figure 3). In *constitutive-expresser of PR genes1* mutants, the overexpression of SA-dependent genes has been efficiently reversed by mutating *SALICYLIC ACID INDUCTION-DEFICIENT2* (*SID2*) (Korasick et al., 2010). To test whether the constitutive expression of *PR* genes we observed in *pub13* plants was SA-dependent, we created homozygous *pub13/sid2* double mutants and compared the expression levels of the *PR1* to *PR5* genes in *pub13*, *sid2*, and wild-type plants. As expected, wild-type and *sid2* plants expressed low levels of the SA-dependent genes compared with the *pub13* mutant (Figure 7B). At the same time, the loss of *SID2* function in the *pub13/sid2* plants was sufficient to block the induction of *PR1*, *PR2*, and *PR5*.

If both *pub13* and *pi4kβ1/pi4kβ2* mutant plants constitutively express SA-dependent *PR* genes, have these plants lost the ability to respond to changes in SA levels? To address this question, we examined whether *pub13* and *pi4kβ1/pi4kβ2* mutants retained the ability to respond to exogenously added SA. In both *pub13* and *pi4kβ1/pi4kβ2* plants, *PR1* gene expression was observed to increase after 24 h of treatment with exogenous SA. While wild-type plants showed a 56-fold increase in *PR1* expression at 24 h after SA treatment, *pub13* and *pi4kβ1/pi4kβ2* plants displayed constitutively increased PR gene expression. These plants retained the ability to respond to SA, as *PR1* gene expression increased by 1.6- and 3.2-fold at the same time point, respectively (Figure 7C). These results indicate that the induction of *PR* genes in *pub13* and *pi4kβ1/pi4kβ2* plants can still be regulated by SA levels.

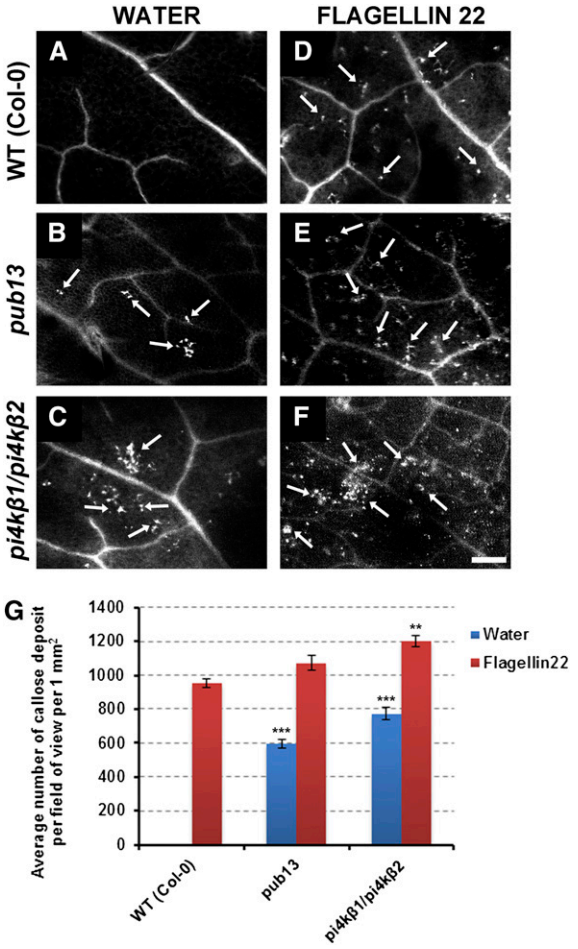

Figure 6. *pub13* and *pi4kβ1/pi4kβ2* Mutant Plants Are No Longer Able to Specifically Induce Callose Deposition.

(A) to **(F)** Leaves of wild-type (Col-0), *pub13*, and *pi4kβ1/pi4kβ2* plants were stained to show basal levels of deposition of callose (**[A]**, **[B]**, and **[C]**, respectively); the same genotypes also were treated with 5 μM flg22 (**[D]**, **[E]**, and **[F]**, respectively). Arrows indicate deposited callose. Bar = 100 μm.

(G) Average numbers of callose deposits per field of view. The results are from three independent experiments, with SD indicated by error bars (n = 15). Asterisks indicate significant differences at $P < 0.05$ (**) and $P < 0.01$ (***) between wild-type (Col-0) and *pub13* plants or between wild-type (Col-0) and *pi4kβ1/pi4kβ2* plants. P values were calculated by Student's t test.

Loss of *FLS2* Function Suppresses the Constitutive SA-Mediated Defense Responses in *pub13* Mutants

A key molecule in the innate immunity of Arabidopsis to *Pst* DC3000 is the receptor protein FLS2, which localizes on the plasma membrane and associates with bacterial flg22 (Chinchilla et al., 2006). Upon binding the flg22 peptide, FLS2 initiates the immune signaling pathways associated with the regulation of *PR* genes

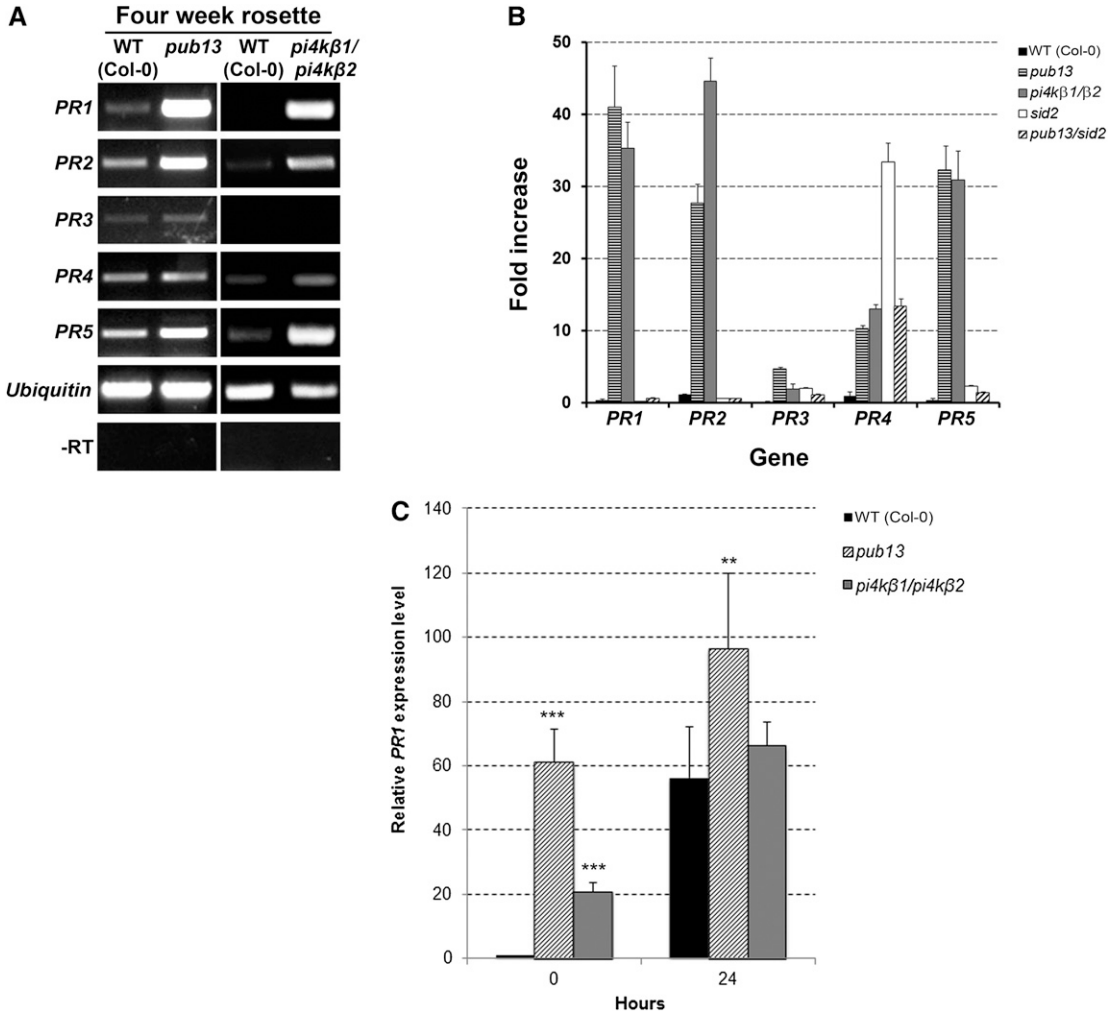

Figure 7. PUB13 and PI4Kβ1/PI4Kβ2 Are Involved in the Expression of the SA-Mediated Defense Response.

(A) and **(B)** RT-PCR **(A)** and qRT-PCR **(B)** analyses of *PR* gene expression in wild-type (Col-0), *pub13*, and *pi4kβ1/pi4kβ2* plants. The mutant genotypes showed a constitutive expression of SA-mediated *PR1*, *PR2*, and *PR5* genes.

(C) qRT-PCR analysis of *PR1* gene expression in wild-type (Col-0), *pub13*, and *pi4kβ1/pi4kβ2* plants upon 2 mM SA treatment. The results are from four technical replicates and three independent experiments, with SD indicated by error bars. Asterisks indicate significant differences at $P < 0.05$ (**) and $P < 0.01$(***) between wild-type (Col-0) and *pub13* plants or between wild-type (Col-0) and *pi4kβ1/pi4kβ2* plants. P values were calculated by Student's *t* test.

(Gomez-Gomez and Boller, 2000; Gómez-Gómez et al., 2001). The loss of *FLS2* results in insensitivity to flg22, leading to an increased sensitivity to pathogenic microorganisms such as *Pst* DC3000. Both *pub13* and *pi4kβ1/pi4kβ2* mutant plants were sensitive to added flg22 (Figure 6), which shows that *FLS2*-mediated pathogen-related signaling still occurs in these plants. To test for a genetic interaction between PUB13 and FLS2, we generated *pub13/fls2* plants and quantified the expression of *PR1* to *PR5* genes in these plants (Figure 8). We found that the simultaneous loss of *PUB13* and *FLS2* genes in the *pub13/fls2* double mutant attenuates the *PR* gene overexpression observed in the *pub13* mutant alone, reducing the overexpression observed when compared with *pub13* (Figure 8B). Thus, the increased expression of *PR* genes in *pub13* plants may be mediated, in part, by upregulation of the FLS2 pathway. Furthermore, the growth defects observed in *pub13* mutants were largely restored to wild-type levels in the *pub13/fls2* double mutants (Figures 8C to 8E).

PUB13 Interacts with Phosphoinositides

As part of the regulation of the membrane trafficking between the Golgi and the plasma membrane, RabA4B recruits the closely related PI4Kβ1 and PI4Kβ2 lipid kinases, and the generation and turnover of the phosphoinositide PI-4P on these membrane compartments play important roles during the regulation of polarized membrane trafficking in Arabidopsis (Preuss et al., 2006). In animals, Rab5 recruits lipid kinases to generate phosphatidylinositol

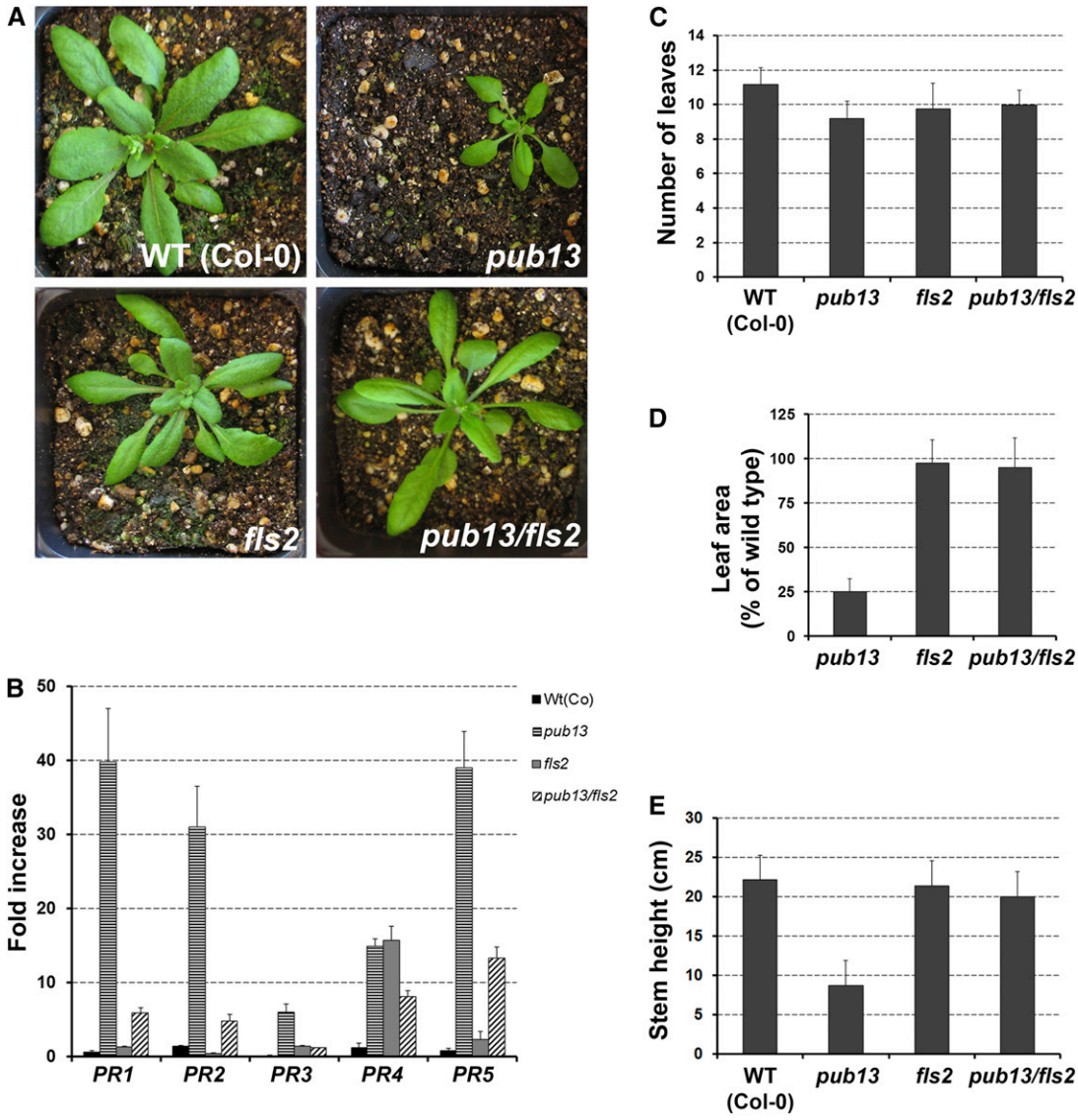

Figure 8. The Loss of FLS2 Restores the Wild-Type Phenotype in *pub13* Mutant Plants.

(A) Aerial view of 24-d-old wild-type (Col-0), *pub13*, *fls2*, and *pub13/fls2* plants.
(B) qRT-PCR analyses of *PR* gene expression in wild-type (Col-0), *pub13*, *fls2*, and *pub13/fls2* plants.
(C) Number of leaves in 4-week-old plants (n = 30 for each genotype).
(D) Leaf surface area calculated for 30 leaves harvested from six individual plants.
(E) Stem height in 4-week-old plants (n = 30 for each genotype).
The data are shown as means ± SD.

3-phosphate (PI-3P) in endosomal membranes (Christoforidis et al., 1999b), and a number of Rab5-interacting proteins are recruited in a dual Rab5- and PI-3P-dependent manner (Simonsen et al., 1998; Nielsen et al., 2000; Zerial and McBride, 2001). We decided to test whether the recruitment of PUB13 by RabA4B might also involve coordinated recruitment through interaction with both RabA4B and phosphoinositides. PUB13 was subdivided into two parts corresponding to the C-terminal ARM-repeat domain and the N-terminal UND-U-box domain. Glutathione *S*-transferase (GST)-tagged versions of the UND-U-box and ARM domains were expressed and purified from *Escherichia coli*, and each of these was tested in a lipid blot assay; we used the Pleckstrin homology (PH) domain of the human protein FOUR-PHOSPHATE-ADAPTOR PROTEIN1 (FAPP1) as a positive control for the binding specificity (Figure 9A). We did not observe any interaction between the UND-U-box domain and lipids (Figure 9B), but surprisingly, we found that the ARM-repeat domain interacts with several different phosphoinositides, especially with PI-4P and phosphatidylinositol 3,4,5-triphosphate (Figure 9C). Similar results were observed in an in vitro liposome binding assay,

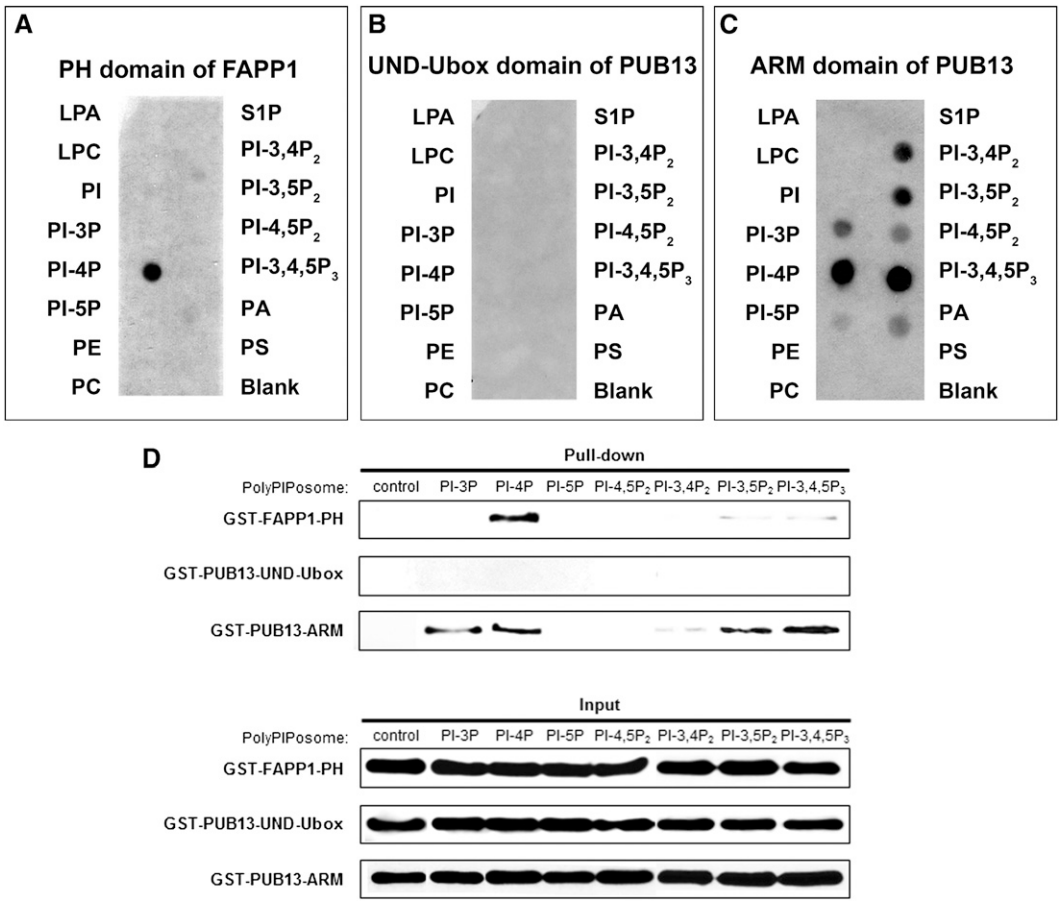

Figure 9. The ARM Repeat of PUB13 Is a Lipid Binding Domain.

(A) The UND-U-box domain and the ARM domain of PUB13 were tested in a lipid blot assay. The PH domain of the human protein FAPP1 was used as a control for the binding specificity in this assay.

(B) and **(C)** The UND-U-box domain did not show any interaction with phosphatidylinositol-phosphates **(B)**, while the ARM domain interacted with multiple phosphoinositides **(C)**.

(D) PolyPIPosome assays with GST-tagged FAPP1-PH, PUB13-UND-U-box, and PUB13-ARM. FAPP1-PH and PUB13-ARM showed binding to PI-4P.

LPA, lysophosphatidic acid; LPC, lysophosphatidylcholine; PA, phosphatidic acid; PC, phosphatidylcholine; PE, phosphatidylethanolamine; PI, phosphatidylinositol; PI-3,4P_2, phosphatidylinositol 3,4-bisphosphate; PI-3,4,5P_3, phosphatidylinositol 3,4,5-triphosphate; PI-3,5P_2, phosphatidylinositol 3,5-bisphosphate; PI-4,5P_2, phosphatidylinositol 4,5-bisphosphate; PS, phosphatidylserine; S1P, sphingosine 1-phosphate.

where the PUB13-ARM domain displayed binding to PI-3P, PI-4P, PI-3,5-diphosphate, and PI-4,5-triphosphate (Figure 9D). We did not observe any interaction between the UND-U-box domain and phosphatidylinositol-containing liposomes (Figure 9D).

DISCUSSION

PUB13 has been previously implicated in the regulation of SA-dependent innate immunity responses in Arabidopsis (Lu et al., 2011; Li et al., 2012a). In this study, we have determined that PUB13 is a RabA4B-interacting protein and show that two previously characterized RabA4B-interacting proteins, the PI4Kβ1 and PI4Kβ2 lipid kinases, also are involved in the regulation of SA-mediated defense responses in Arabidopsis. Furthermore, we observed that PUB13 interacts with phosphoinositides, including PI-4P, through its C-terminal ARM domain. These results demonstrate that RabA4B-dependent trafficking pathways play important roles in the regulation of SA-dependent innate immunity responses in Arabidopsis.

Recent studies on the flagellin receptor protein FLS2 and pathogen-triggered immunity revealed that the expression of SA-dependent genes is negatively regulated by the U-box protein PUB13 in noninfected plants (Lu et al., 2011; Li et al., 2012a). Indeed, loss of PUB13 results in uncontrolled expression of *PR1*, accumulation of SA, and constitutive resistance to pathogenic bacteria (Li et al., 2012a), observations that we independently confirmed here (Figures 5 to 7). Constitutive expression of these *PR* genes in *pub13* plants is dependent upon SA accumulation, as these effects could be efficiently reversed in *pub13/sid2* double mutants (Figure 7B). According to the model proposed

by Lu et al. (2011), the degradation of FLS2 requires the specific E3 ligase activity of PUB13, and its homolog PUB12, to interact with the FLS2 coreceptor BRASSINOSTEROID INSENSITIVE (BRI1)-ASSOCIATED RECEPTOR KINASE1 (BAK1). BAK1 interacts directly with FLS2 in a flg22-dependent fashion, and formation of the FLS2-BAK1-PUB13/12 complex results in turnover of the FLS2 receptor (Lu et al., 2011). Our results support the hypothesis that PUB13 is a negative regulator of SA-dependent gene expression and defense response and further identify that PUB13 is recruited to Golgi-associated TGN compartments, at least in part through its interaction with RabA4B (Figure 3). Consistent with an important role for RabA4B in regulating FLS2-mediated defense responses, we show that two other previously identified RabA4B-interacting proteins, PI4Kβ1 and PI4Kβ2, also are involved in negatively regulating the expression of SA-dependent *PR* genes.

Importantly, we demonstrated that the constitutive activation of SA-mediated defense responses was significantly reduced in *pub13/fls2* plants (Figure 8) and that overall growth defects observed in *pub13* mutants were largely restored to the wild type in the *pub13/fls2* double mutant background (Figures 8A, 8D, and 8E; Supplemental Figure 1B). These findings indicate that the enhanced expression of *PR* genes and associated growth phenotypes observed in *pub13* are, at least in part, directly dependent upon signaling through the FLS2 receptor protein. The FLS2 receptor normally functions to bind and detect the bacterial flagellin protein (Gomez-Gomez and Boller, 2000; Gómez-Gómez et al., 2001). A common defense response initiated by flagellin or flg22 treatment is callose deposition. Our results indicated that both *pub13* and *pi4kβ1/pi4β2* mutant plants had positive callose staining after treatment with flg22 (Figure 6). These results support the idea that the FLS2 receptor is present and functional in both *pub13* and *pi4kβ1/pi3kβ2* mutant plants.

More recently, FLS2 has been shown to continuously cycle between the plasma membrane and internal compartments (Beck et al., 2012), and these studies have indicated that the recycling of internalized FLS2 undergoes two distinct endocytic pathways, according to the activation status of the receptor (nonelicited versus elicited). These results imply that the propensity of flg22-FLS2 and nonelicited FLS2 complexes to activate defense-related signaling pathways is associated with altered subcellular sorting of the FLS2 receptor either for degradation or recycling back to the plasma membrane. This would be compatible with our observation that PUB13 localizes to an internal Golgi-associated TGN compartment (Figure 3), where its interaction with FLS2 may be associated with productive sorting of this receptor protein into either the degradative or recycling membrane trafficking pathway. Interestingly, the expression of mutant forms of different members of the RabA4 GTPase family was recently shown to affect endocytosis, sorting, and recycling events associated with TGN and multivesicular body compartments (Choi et al., 2013). Additionally, RabA4C, which shares a high degree of sequence similarity with RabA4B, has been implicated in regulation of the callose synthase POWDERY MILDEW RESISTANT4, further highlighting an important role for RabA GTPases during plant defense signaling (Ellinger et al., 2014). Combining these earlier results with our observations, we propose a working model for the function of RabA4B-recruited PI4Kβ1 (and PI4Kβ2) and PUB13 during the subcellular trafficking of FLS2 (Figure 10). In our working model, we suggest that RabA4B-recruited PUB13 and PI4Kβ1/β2 proteins function in the normal sorting of the internalized FLS2 protein (Figure 10) and that loss of these protein functions would result in altered subcellular dynamics of either empty FLS2 protein or flg22-FLS2 complexes (Figure 10). In particular, we suggest in our model that the RabA4B recruitment of PI4K activities assists in the enrichment of PI-4P on Golgi-associated TGN compartments and that this in turn assists in the recruitment of other proteins, such as PUB13, that participate in the appropriate sorting and activity of FLS2 and other potential elements associated with SA-dependent defense signaling (Figure 10).

Rab GTPases regulate aspects of membrane trafficking through the GTP-dependent recruitment of cytosolic proteins (Zerial and McBride, 2001; Grosshans et al., 2006; Hutagalung and Novick, 2011). RabA4B was shown previously to recruit two closely related lipid kinases, PI4Kβ1 and PI4Kβ2 (Preuss et al., 2006), and the generation and turnover of the phosphoinositide PI-4P was shown to play important roles during polarized membrane trafficking in tip-growing cells (Thole and Nielsen, 2008; Szumlanski and Nielsen, 2009). PUB13, like PI4Kβ1 and PI4Kβ2, specifically interacts with RabA4B in its active, GTP-bound state (Figure 1A), and a functional EYFP-PUB13 fluorescent fusion displays significant colocalization with RabA4B on Golgi-associated membrane compartments in both root and leaf epidermal cells (Figures 3C and 3F). Significantly, however, EYFP-PUB13 was not observed to accumulate on apical vesicle populations in tip-growing root hair cells (Supplemental Movie 1), as has been shown for both RabA4B and PI4Kβ1 (Preuss et al., 2004, 2006). These results are consistent with the observation that T-DNA insertional mutants of PUB13 failed to display root hair growth defects (Figure 4) and indicate that, unlike PI4Kβ1 and PI4Kβ2, PUB13 does not appear to play essential roles during polarized membrane trafficking during tip-restricted expansion in these cells. Instead, colocalization between PUB13 and RabA4B appears to be restricted to Golgi-associated membranes (Figures 3I and 3L) also labeled by the Golgi-localized SYP32 marker (Geldner et al., 2009). RabA4B labels budding vesicle profiles on Golgi-associated TGN compartments as well as independent vesicles derived from these membranes (Kang et al., 2011). We interpret these results as an indication that RabA4B interaction with PUB13 is limited to Golgi-associated TGN elements and that, unlike PI4Kβ1, the association between RabA4B and PUB13 is not maintained once RabA4B vesicles have finished budding from these Golgi-associated TGN compartments (Figure 10).

In some instances, the efficient recruitment of Rab-GTPase-interacting proteins to a particular membrane compartment involves direct interaction with both the Rab-GTPase and the membranes of that compartment through lipid-interacting domains that can recognize one or more classes of phosphoinositide lipids (Simonsen et al., 1998; Zerial and McBride, 2001). During endosomal trafficking in animals, the Rab-GTPase Rab5 recruits PI3Ks to enrich endosomal membranes for PI-3P (Christoforidis et al., 1999b), which in turn facilitates the recruitment of a number of Rab5-interacting proteins that also contain the PI-3P binding domains, such as EARLY ENDOSOME ANTIGEN1, Rabenosyn-5, and Rabankyrin-5 (Simonsen et al., 1998; Christoforidis et al., 1999a; Nielsen et al., 2000; Schnatwinkel et al., 2004; Stenmark, 2009). PI-3P also has been shown to be enriched in plant compartments associated with endocytosis, although whether these

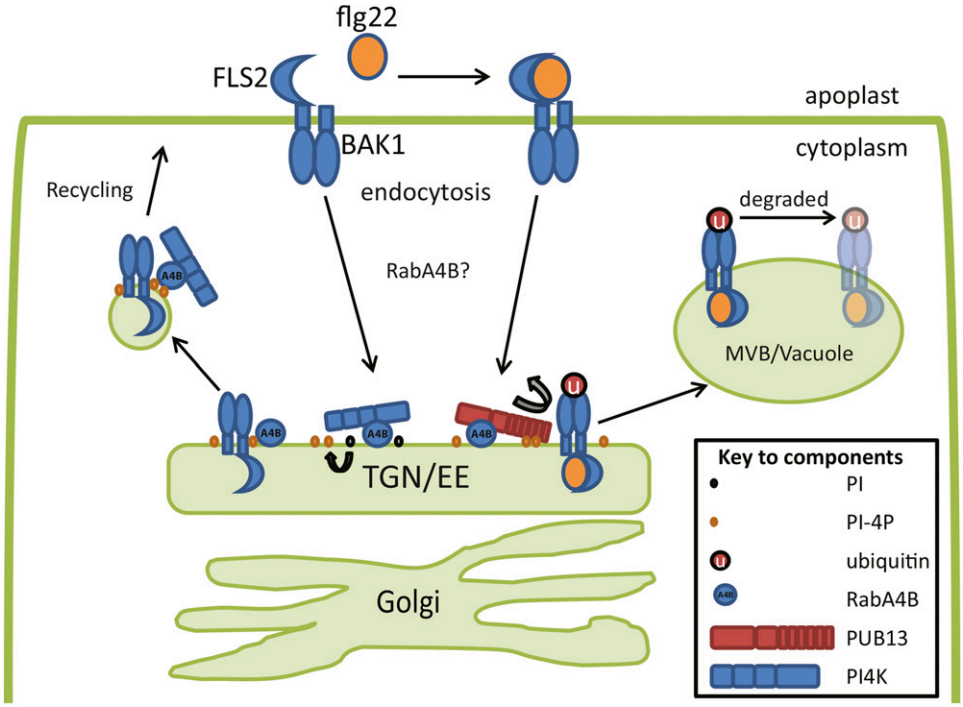

Figure 10. Model for the RabA4B-Mediated Recruitment of PUB13 and PI4Kβ1/β2 to Regulate the Plant Defense Response.

FLS2-BAK1 complexes localize predominantly at the plasma membrane in nonelicited cells, but this complex continuously cycles between plasma membranes and internal TGN/early endosome (TGN/EE) compartments in nonelicited cells. These TGN/EE compartments are enriched for PI-4P through the recruitment of PI4Kβ1 (and PI4Kβ2) by active RabA4B. The presence of RabA4B and PI-4P recruits PUB13 as well as other PI-4P binding proteins to these TGN/EE compartments. In nonelicited cells, RabA4B and RabA4B-recruited PI4Kβ1 (and PI4Kβ2) participate in the rapid recycling of FLS2-BAK1 complexes to the plasma membrane. Upon elicitation with flg22, flg22-FLS2-BAK1 complexes are rapidly internalized and ubiquitinated by PUB13 in TGN/EE compartments containing RabA4B and RabA4B-recruited PI4Kβ1 (and PI4Kβ2). Loss of PI-4P and/or PUB13 on RabA4B-associated TGN/EE compartments interferes with the recycling of FLS2-BAK1 to the plasma membrane (nonelicited cells) or the sorting and turnover of flg22-FLS2-BAK1 complexes in multivesicular body (MVB)/vacuole compartments (elicited cells).

represent early or late endocytic compartments remains unclear (Voigt et al., 2005; Robinson et al., 2008). Intriguingly, in plants, early endosomal compartments involved in the recycling of internalized plasma membrane proteins such as BRI1, PIN-FORMED proteins, and FLS2 appear to be associated with compartments labeled by RabA-GTPase family members (Feraru et al., 2012; Choi et al., 2013). These RabA-labeled membranes, which emerge from Golgi-associated TGN compartments (Kang et al., 2011), also appear to play significant roles in the polarized secretion of new cell wall components, both in tip-growing cells and in cells undergoing cytokinesis, suggesting that at least in some cases there may be significant overlap between membrane trafficking compartments involved in endocytic recycling and in polarized secretion in plants. Intriguingly, RabA4B, which was shown previously to regulate polarized membrane-trafficking events in tip-growing cells (Preuss et al., 2004; Szumlanski and Nielsen, 2009), recruits the lipid kinases PI4Kβ1 and PI4Kβ2, and the production and regulation of PI-4P levels in these membranes play important roles during the regulation of membrane-trafficking events (Walch-Solimena and Novick, 1999; Audhya et al., 2000; Li et al., 2002; Godi et al., 2004; Preuss et al., 2006; Thole and Nielsen, 2008). Our data showed that the ARM repeat domain of PUB13 shows significant binding to phosphoinositides, in particular to PI-4P. While PUB13 did display binding to some other phosphatidylinositol isoforms, phosphatidylinositol 4,5-bisphosphate is thought to be mainly localized to the plasma membrane (Mueller-Roeber and Pical, 2002; Lee et al., 2007) while phosphatidylinositol 3,4-bisphosphate and phosphatidylinositol 3,4,5-triphosphate have not been detected in plants (Mueller-Roeber and Pical, 2002; Furt et al., 2010), excluding the possibility that either of these lipids interacts with PUB13 at the TGN. PI-4P was shown to localize to the TGN membrane (Wang et al., 2003). Therefore, it is likely that PUB13 interacts specifically with PI-4P in vivo. These results would be consistent with a model in which RabA4B recruitment of PI4Kβ1 (and PI4Kβ2) lipid kinases results in the localized accumulation of PI-4P, which creates a membrane microenvironment suitable for the recruitment of PUB13. Intriguingly, the ENHANCED DISEASE RESISTANCE2 (EDR2) protein also has been shown to contain a PH domain that binds specifically to PI-4P, and *edr2* mutant plants also display constitutively activated SA defense responses (Vorwerk et al., 2007). This raises the interesting possibility that the ability to bind PI-4P may be common to multiple proteins involved in the appropriate regulation of SA-mediated defense responses in Arabidopsis.

Our data provide additional insight into the functions of some of the domains of PUB13. Although the UND in *Brassica* ARC1 was

used previously to isolate its interacting protein (Samuel et al., 2009), the UND in PUB13 is an uncharacterized plant-specific domain unique to PUB proteins (Mudgil et al., 2004). The U-box domain has been characterized as a putative E3 binding domain (Aravind and Koonin, 2000; Hatakeyama et al., 2001; Ohi et al., 2003), which is necessary for the ubiquitination of target proteins (Aravind and Koonin, 2000; Hatakeyama et al., 2001). Recently, the SPL11 U-box domain was shown to be important for the interaction with E2 (Bae and Kim, 2013), and in this class of proteins, this domain has been shown to be essential to trigger disease resistance in tobacco (*Nicotiana tabacum*) and tomato (*Solanum lycopersicum*) (González-Lamothe et al., 2006). We found that the UND-U-box domain was important for the interaction between PUB13 and RabA4B, perhaps supporting a role for UND in mediating protein-protein interactions. ARM repeats have been described previously as protein-protein interaction domains (Coates, 2003). In this study, we found that the ARM repeat domain of PUB13 has a propensity to interact with phosphoinositides. Structural studies of the ARM repeat domain have indicated significant structural similarity to Epsin NH_2-Terminal (ENTH) domains (Hyman et al., 2000). ENTH domains have been widely characterized as having phosphatidylinositol binding capacity (De Camilli et al., 2002) and participate in vesicle-trafficking events (Itoh et al., 2001). We propose that PI-4P generation by PI4Kβ1/β2 might result in the generation of a membrane microenvironment suitable for the recruitment of other RabA4B-interacting proteins. Targeting of PUB13 and possibly other cytosolic proteins to this PI-4P-enriched domain may play important roles in the sorting of signaling components, such as the FLS2 receptor, between degradation in late endosomal and vacuolar compartments or recycling back to the plasma membrane (Figure 10) (Robatzek et al., 2006; Salomon and Robatzek, 2006; Göhre et al., 2008; Beck et al., 2012).

METHODS

Construction of Clones and Y2H Interaction Assays

The yeast strain AH109 (Clontech Laboratories) was used for testing protein interactions. GTP-bound and GDP-bound forms of RabA4B, RabG3C, RabF2A, and ROP1 were generated and cloned into the pGBKT7 bait vector as described (Preuss et al., 2006). Sequencing of the original *PUB13* clone identified in the Y2H assay determined that it corresponded to amino acids 1 to 551. Protein domains of PUB13 were cloned using primers specific to the UND (5′-CATGCCATGGAGGAAGAGAAAGCTTCTGCT-3′ and 5′-CCGGAATTCAGTCTGTCCATTGCTTCTAGA-3′), U-box (5′-CCGGAATTCTCTACGGCAGCGAGTCAGAAG-3′ and 5′-GCGGATCCTTGGTCCTCGGGGTTTCCGTA-3′), ARM (5′-CCGGAATTCCGATCTGCAGCTGGGGAAATC-3′ and 5′-CCGCTCGAGTTAAGTATCTGCAGCTTCTGT-3′), UND-U-box domains (5′-CATGCCATGGAGGAAGAGAAAGCTTCTGCT-3′ and 5′-GCGGATCCTTGGTCCTCGGGGTTTCCGTA-3′), U-box-ARM domains (5′-CCGGAATTCTCTACGGCAGCGAGTCAGAAG-3′ and 5′-CCGCTCGAGTTAAGTATCTGCAGCTTCTGT-3′), and full-length PUB13 (5′-CATGCCATGGAGGAAGAGAAAGCTTCTGCT-3′ and 5′-CCGCTCGAGTTAAGTATCTGCAGCTTCTGT-3′).

The pGBKT7-RabA4B clones and pGADT7-PUB13 domain clones were transformed into yeast using a LiAc-mediated transformation method (Gietz and Woods, 1994). Two-milliliter liquid cultures, selecting for the presence of plasmid(s) of interest, were grown for 2 d at 30°C at 260 rpm. Cultures were diluted to an OD_{600} of 0.02, and 10 μL droplets were placed onto selective and nonselective media. Plates were scanned after 7 d of growth at 30°C.

Protein-Protein Direct Interaction Assay

A far-western protein gel blot assay (Walsh et al., 2012) was conducted to assess the interaction between PUB13 and RabA4B. Briefly, the GST-tagged PUB13 was expressed and purified from BL21DE *Escherichia coli* cells, and a serial dilution of the protein was applied to a precut, dry nitrocellulose membrane. GST alone was added to the membrane as a negative control. The membrane was shaken in 10 mL of blocking buffer at room temperature. After 1 h, the blocking buffer was removed and replaced with protein binding buffer containing GTP-bound (GTPγS) RabA4B, and the membrane was incubated at 4°C. After 6 h of incubation on a rotary shaker, the membrane was washed three times with blocking buffer and placed in 10 mL of blocking buffer containing anti-RabA4B antibody (1:10,000 dilution) overnight at 4°C on an orbital shaker. The primary antibody solution was removed, and the membrane was washed three times with blocking buffer and incubated for 3 h with 10 mL of blocking buffer containing anti-rabbit horseradish peroxidase secondary antibody (1:2000 dilution). After incubation with the secondary antibody, the membrane was washed once with blocking buffer and twice with protein dilution buffer. The blot was activated by the addition of 1 mL of each component of the chemiluminescent substrate.

BiFC and Quantification

The interaction between PUB13 and the constitutively active form (GTP-bound) of RabA4B was verified in a structural complementation assay using pSAT1- and pSAT4-derived plasmids (Citovsky et al., 2006) for transient expression of the fusion proteins in *Nicotiana benthamiana* (Sparkes et al., 2006). The C-terminal end of PUB13 was fused to the N-terminal moiety or to the C-terminal moiety of YFP (nYFP or cYFP, respectively), while for RabA4B, the fluorescent tags were added to the N-terminal end of the protein to prevent potential interference with the mutation in the C-terminal CAAX box. Two days after injection with *Agrobacterium tumefaciens* GV3101, leaf tissues were treated with propidium iodide (10 μg/mL solution) to stain the outline of the cells and viewed with an Olympus spinning disc confocal microscope equipped with two laser lines and a set of filters capable of distinguishing between YFP and RFP. The samples were observed under 20× magnification (Olympus UPLSAPO20X; NA = 0.70). To excite the YFP, we used a 515-nm/50-mW diode laser; to excite phosphatidylinositol, we used a 561-nm/50-mW diode laser. Quantitation of the fluorescence intensities from BiFC experiments was performed on representative images from five independent leaves transiently expressing nYFP and cYFP constructs. To determine relative BiFC fluorescence, 10 regions of 2×10^{-3} mm^2 were selected for each image, and the relative fluorescence intensity of these regions was determined using ImageJ. These values were averaged to obtain the fluorescence intensity for each of the five independent images examined. BiFC values for each leaf were normalized by comparison with corresponding phosphatidylinositol fluorescence values.

Characterization of *PUB13* Insertion Mutant and *SID2* Deletion Mutant

The *PUB13* insertion mutant was obtained from the SALK T-DNA collection (SALK_093164; ABRC). The T-DNA insertion site in *PUB13* was confirmed by sequencing the T-DNA junction using primers specific to *PUB13* (5′-ATCGGGTACCATGGAGGAAGAGAAAGCTTCTG-3′ and 5′-ATCGGAGCTCTTAAGTATCTGCAGCTTCTGTGG-3′) and to the left border of the T-DNA (5′-GCGTGGACCGCTTGCTGCAACT-3′). The insertion site consists of a head-to-head insertion of two copies of the T-DNA. Sequencing of both sides of the T-DNA insert confirmed that it is located in the third exon of *PUB13* at base pair 1045 of the genomic sequence. The *sid2* mutant seeds were obtained from Antje Heese's laboratory (University of Missouri). The mutation consists of a deletion and was detected using primers flanking the deletion site (5′-TTCTTCATGCAGGGGAGGAG-3′, 5′-CAACCACCTGGTGCACCAGC-3′, and 5′-AAGCAAAATGTTTGAGTCAGCA-3′). Double mutant

pub13/sid2 plants were obtained by crossing the two parental lines together and genotyping for double homozygous mutant plants in the F2 generation.

Generation of Transgenic Lines Coexpressing EYFP-PUB13/ECFP-RabA4B and EYFP-PUB13/RFP-SYP32

The full-length *PUB13* domain was amplified from wild-type cDNA using primers specific to *PUB13* (forward primer, 5′-CATGCCATGGAGGAAGA-GAAAGCTTCTGCT-3′; reverse primer, 5′-CCGCTCGAGTTAAGTATCTG-CAGCTTCTGT-3′). The insert was cloned into the plant transformation vector pCAMBIA (CAMBIA) containing a 35S promoter element used to drive the expression of EYFP, thus creating pCAM-35S-EYFP-PUB13 vector. Wild-type *Arabidopsis thaliana* (Col-0) plants were transformed by floral dipping (Clough and Bent, 1998). Independent transformants were selected by growth on hygromycin and then transplanted to soil. Independent T3 lines were used for imaging. Homozygous transgenic 35S-EYFP-PUB13 plants were crossed with the transgenic line expressing CFP-RabA4B. The F1 progeny were selected on one-quarter-strength Murashige and Skoog plates containing hygromycin (50 μg/mL). Resistant F1 seedlings were analyzed by confocal microscopy for the expression of the EYFP and CFP fusion proteins. Homozygous transgenic 35S-EYFP-PUB13 plants were crossed with the transgenic line generated by Geldner et al. (2009) expressing the marker RFP-SYP32. The F1 progeny were selected on one-quarter-strength Murashige and Skoog plates containing hygromycin (50 μg/mL) and kanamycin (30 μg/mL), and the double resistant F1 seedlings were analyzed by confocal microscopy for the expression of the EYFP and RFP fusion proteins.

RT-PCR Analysis of *PUB13* Expression

Leaves of wild-type (Col-0) and *PUB13* homozygous mutant (*pub13*) plants were collected and frozen in liquid nitrogen. Total RNA was extracted from each sample using the Qiagen RNeasy Kit. Total cDNA was synthesized from each RNA sample using the Invitrogen SuperScript III First-Strand Synthesis System for RT-PCR and the oligo(dT) primer according to kit instructions. Reactions with primers specific to *UBIQUITIN10* (5′-TGCCGGAAAACAATTGGAGGATGG-3′ and 5′-CGTACTTTGGCCGACTACAACATC-3′) were used to equalize the amounts of cDNA from the different sources. PCR was performed with GoTaq Green (Promega) using primers specific to *PUB13* (5′-CCGGAATTCC-GATCTGCAGCTGGGGAAATC-3′ and 5′-CCGCTCGAGTTAAGTATCTG-CAGCTTCTGT-3′). The amplification program consisted of 30 s at 94°C, 30 s at 56°C, and 1 min at 68°C for 28 cycles, followed by a 10-min extension at 68°C. PCR products were visualized on an agarose gel using ethidium bromide.

PR Gene Expression Analysis by RT-PCR

Plants were grown in soil for 4 weeks, and rosettes from 4-week-old plants were collected and frozen in liquid nitrogen. Total RNA was extracted from each sample using the Qiagen RNeasy Kit. The cDNA was synthesized from each RNA sample using the Invitrogen SuperScript III First-Strand Synthesis System for RT-PCR using oligo(dT) primer according to kit instructions. Reactions with primers specific to *UBIQUITIN10* (5′-GATCTTTGCCGGAAAACAATTGGAGGATGGT-3′ and 5′-CGACTTGTCAT-TAGAAAGAAAGAGATAACAGG-3′) were used to equalize amounts of cDNA from the different sources. PCR was performed with GoTaq Green (Promega) using primers specific to *PR1* (5′-CGTCTTTGTAGCTCTTGTAGGTGC-3′ and 5′-GTATGGCTTCTCGTTCACATAATTCCC-3′), *PR2* (5′-ATGTCTGAAT-CAAGGAGCTTAGCC-3′ and 5′-GTTGAGACCTTGACTTCAAGCC-3′), *PR3* (5′-CCGAGCAATGTGGTCGCC-3′ and 5′-CCGTAGTAGCGTTTGC-CAG-3′), *PR4* (5′-CGCGCCACCTACCATTTCTA-3′ and 5′-TCAAACGC-GATCAATGGCCGA-3′), and *PR5* (5′-CTCTTCCTCGTGTTCATCACAA-3′ and 5′-GTTGAGGTCAGAGACACAGCC-3′). Reactions lacking reverse transcriptase were used to detect the presence of any contaminating genomic DNA. The amplification program consisted of 30 s at 94°C, 30 s at 59°C, and 1 min at 68°C for 28 cycles, followed by a 10-min extension at 68°C. PCR products were visualized on an agarose gel using ethidium bromide.

qRT-PCR Analysis of *PR* Gene Expression

Plants were grown in soil for 4 weeks, and rosettes were harvested and frozen in liquid nitrogen. Total RNA was extracted from each sample using the Qiagen RNeasy Kit. cDNA was synthesized from each RNA sample using the Invitrogen SuperScript III First-Strand Synthesis System for RT-PCR using oligo(dT) primer according to kit instructions. PCR was performed using SybrGreen (Bio-Rad). Reactions were run in a Bio-Rad iCycler using iQ SYBR Green Supermix (Bio-Rad) with primers specific to *UBIQUITIN10* (5′-GGAAAGCTCCGACACCATTG-3′ and 5′-CAAGCTGCTTTCCAGCGAAG-3′) serving as a standard. Reactions without reverse transcriptase were used to detect the presence of contaminating genomic DNA. Relative gene expression levels were obtained using primers specific to *PR1* (5′-GAGGAGCGGTAGGCGTAGGT-3′ and 5′-CCGCTACCCCAGGCTAAGTT-3′), *PR2* (5′-AAGTCCATCGGACGTTGTGG-3′ and 5′-ACTGGGAACGTC-GAGGATGA-3′), *PR3* (5′-TGGATTGGAGTGTGGACGTG-3′ and 5′-AG-GAGGCCGTTAACGAAGGA-3′), *PR4* (5′-ACGGAGGCTTGGATTTGGAT-3′ and 5′-GAATCAGGCTGCCCAATGAG-3′), and *PR5* (5′-TCGGGA-GATTGCAAATACGC-3′ and 5′-ACTCTTGCAGGCCACGACAT-3′). The cycle consisted of three repeats of 95°C for 30 s, a 95°C hold for 3 min, followed by 50 repeats of the following amplification cycle: 95°C for 15 s, 62°C for 30 s, and 72°C for 30 s. After a final hold at 95°C for 1 min, the samples were cooled to 55°C and incrementally raised to 95°C for a melt-curve analysis. Reactions were tested in triplicate, and similar results were obtained in three separate experiments.

Aniline Blue Staining of Leaves for Detection of Callose Deposition

To visualize the induction of callose deposition, leaves from 4-week-old plants were injected with 1 μM flg22 and stained after 12 h as described before (Korasick et al., 2010). Briefly, the leaf tissue was fixed overnight in 1% glutaraldehyde, 5 mM citric acid, and 90 mM Na_2HPO_4, pH 7.4, cleared, and dehydrated with 100% ethanol. Cleared tissue was transferred sequentially in 50% ethanol and in 67 mM K_2HPO_4, pH 12, and then stained for 1 h at room temperature in 0.01% aniline blue in 67 mM K_2HPO_4, pH 12. Leaves injected with water alone were used as a negative control. Stained material was mounted in 70% glycerol and 30% stain and examined using UV epifluorescence (Nikon E600) with fluorescence optics and appropriate filters.

Challenge Experiments with *Pseudomonas syringae* pv *tomato* DC3000

The phytopathological assay was performed according to the protocol described by Ishiga et al. (2011). Briefly, surface-sterilized seeds were grown in a Petri dish (100 mm × 25 mm) under a 12-h-light/12-h-dark photoperiod in environmentally controlled chambers. Two-week-old plants were flood-inoculated with 40 mL of a suspension of *Pst* DC3000 cells (1×10^5 starting concentration), and the rate of bacterial growth inside leaves was measured 0, 2, and 4 d after inoculation. Plants flood-inoculated with water alone were used as a negative control. The numerical value of bacterial growth was normalized to colony-forming units/mg using the total weight of the tissues used for the assay.

Characterization of *pub13/fls2* Mutant Plants

The *fls2* mutant seeds were obtained from TAIR. The mutation consists of a T-DNA insertion in the FLS2 gene (SALK_093905) and was detected using primers flanking the deletion site (5′-CATAAGCTTGAACCTTTCAAGG-AACAG-3′ and 5′-TATCCAGAATGAAGATAATCGATTCCGC-3′). Double

mutant *pub13/fls2* plants were obtained by crossing the two parental lines together and genotyping for double homozygous mutant plants in the F2 generation. The number of leaves in 24-d-old plants, the length of the stem, and the leaf area of *pub13/fls2* plants were measured and compared with wild-type (Col-0), *pub13*, and *fls2* plants. For the leaf area, we measured five leaves for each plant (from leaf 4 to leaf 8) on a total of six plants for each genotype; the surface area was calculated with ImageJ.

Lipid-Protein Binding Assay

The UND-U-box and ARM domains of *PUB13* were cloned in pGEX4T-1 for expression in BL21DE *E. coli* cells, and the purified proteins were used in a lipid binding assay. The lipid binding activity was assessed on PIPs-P6001 strips (Echelon Biosciences). Each strip was placed in a Petri dish containing PBST with albumin (3%) and shaken in darkness at room temperature; after 1 h, the blocking buffer was removed and 10 mL of PBST containing the UND-U-box or ARM protein (0.20 pmol) was added to the Petri dish. The protein was removed after overnight shaking at 4°C, and the membrane was washed three times with PBST (10 min for each wash) before adding 10 mL of PBST containing anti-GST antibody from goat (1:2000 dilution; GE Healthcare). The lipid filter was then incubated on a shaker for 1 h at room temperature and washed three times before adding 10 mL of PBST containing anti-goat IgG antibody from donkey, horseradish peroxidase conjugate (1:7500 dilution; GE Healthcare). The lipid strip was incubated on a shaker at room temperature and after 45 min washed twice with 10 mL of PBST and rinsed in 10 mL of PBS for 10 min. The blot was activated by the addition of 1 mL of each component of the chemiluminescent substrate (Amersham ECL Prime Western Blotting Detection Reagent) and exposed to film for 10 s. For PolyPIPosome experiments, 20 μL of l mM PolyPIPosomes (65% phosphatidylcholine, 29% phosphatidylethanolamine, 1% biotinylated phosphatidylethanolamine, and 5% phosphoinositides; Echelon Biosciences) was mixed with 30 pmol of purified proteins in 1 mL of binding buffer (50 mM Tris-HCl, pH 7.6, 150 mM NaCl, and 0.05% Nonidet P40) and rotated for 90 min at room temperature. Neutravidin beads (20 μL) were added to pull down the lipid-protein mixtures for 1 h at room temperature. The mixture was subsequently centrifuged (2 min, 2500*g*), and supernatant was recovered for input analysis. Following three washes with 1 mL of binding buffer as detailed above, the pellet was resuspended with 2× Laemmli sample buffer followed by analysis by SDS-PAGE and protein gel blotting with antibodies specific to GST (1:1500 dilution), as detailed above.

Microscopic Observations of Fluorescent Proteins

The samples were observed with an Olympus spinning disc confocal microscope equipped with laser lines and a set of filters capable of distinguishing CFP, YFP, and RFP. The samples were observed under 10× (Olympus UPLFLN10X2; NA = 0.3) or 20× (Olympus UPLSAPO20X; NA = 0.70) magnification. To excite the CFP, we used a 445-nm/40-mW diode laser; to excite the YFP, we used a 515-nm/50-mW diode laser; to excite the RFP, we used a 561-nm/50-mW diode laser.

Complementation of *pub13* Mutant Plants

Full-length *PUB13* was amplified from wild-type leaf cDNA and cloned into the pCAM-35S vector and into the pCAM-35S-EYFP vector for stable expression in Arabidopsis. Homozygous *pub13* mutant plants were transformed by floral dipping (Clough and Bent, 1998). Independent transformants were selected by growth on hygromycin and were transplanted to soil. Plants were verified as homozygous *pub13* by PCR using primers specific to the genomic clone of PUB13 (5′-GCTTTGTTTTGCTATGGTAGTGTTTGAG-3′ and 5′-ATCGGAGCTCTTAAGTATCTGCAGCTTCTGTGG-3′) and to the left border of the T-DNA (5′-GCGTGGACCGCTTGCTGCAACT-3′). The presence of 35S-EYFP-PUB13 was confirmed using primers specific to EYFP (5′-CGCCACCATGGTGAGCAAGGGCGAGGAGCT-3′) and to PUB13 (5′-GCGGATCCTTGGTCCTCGGGGTTTCCGTA-3′). The presence of 35S-PUB13 was confirmed using primers specific to the 35S promoter (5′-CCGGAATTCATGGAGTCAAAGATTCAAATA-3′) and to PUB13 (5′-GCGGATCCTTGGTCCTCGGGGTTTCCGTA-3′). The expression of *PR1* in individual complementation plants was tested by qRT-PCR as described above.

Accession Numbers

Sequence data from this article can be found in the Arabidopsis Genome Initiative database under the following accession numbers: *PUB13* (At3g46510), *RabA4B* (At4g39990), *SID2* (At1g74710), *PR1* (At2g14610), *PR2* (At3g57260), *PR3* (At3g12500), *PR4* (At3g04720), *PR5* (At1g75040), *UBIQUITIN10* (At4g05320), *FLS2* (At5g46330), *PI4Kβ1* (At5g64070), and *PI4Kβ2* (At5g09350).

Supplemental Data

Supplemental Figure 1. Characterization of *pub13*, *pub13* Expressing EYPF-PUB13, and *pub13/fls2* Mutant Phenotypes.

Supplemental Figure 2. *PI4Kβ1 D972A* Does Not Rescue *pi4kβ1/pi4kβ2* Phenotypes.

Supplemental Figure 3. Restoration of Wild-Type Levels of *PR1* in Stably Transformed *pub13* Expressing Either *EYFP-PUB13* or Untagged *PUB13* Genes.

Supplemental Movie 1. Mobile EYFP-PUB13 Fusion Protein-Labeled Punctate Structures.

ACKNOWLEDGMENTS

We thank Antje Heese (University of Missouri) for kindly providing the *sid2* seeds. We also thank Gregg Sobocinski of the Department of Molecular, Cellular, and Developmental Biology imaging laboratory of the University of Michigan for microscopy support and Fangwei Gu for technical support and helpful discussions. This work was supported by the Department of Energy (Grant DE-FG02-07ER15887 to E.N., V.A., A.L.K., and G.B.) and the National Science Foundation (Grant 0937323 to E.N.).

AUTHOR CONTRIBUTIONS

E.N. designed the research. V.A., A.L.K., G.B., S.D.C., and T.D. performed the experiments. V.A., A.L.K., and G.B. analyzed the data. V.A., A..L.K., G.B., and E.N. wrote the article.

Received November 13, 2014; revised December 28, 2014; accepted January 9, 2015; published January 29, 2015.

REFERENCES

Aravind, L., and Koonin, E.V. (2000). The U box is a modified RING finger—A common domain in ubiquitination. Curr. Biol. **10:** R132–R134.

Audhya, A., Foti, M., and Emr, S.D. (2000). Distinct roles for the yeast phosphatidylinositol 4-kinases, Stt4p and Pik1p, in secretion, cell growth, and organelle membrane dynamics. Mol. Biol. Cell **11:** 2673–2689.

Bae, H., and Kim, W.T. (2013). The N-terminal tetra-peptide (IPDE) short extension of the U-box motif in rice SPL11 E3 is essential for

the interaction with E2 and ubiquitin-ligase activity. Biochem. Biophys. Res. Commun. **433:** 266–271.

Bardoel, B.W., van der Ent, S., Pel, M.J.C., Tommassen, J., Pieterse, C.M.J., van Kessel, K.P.M., and van Strijp, J.A.G. (2011). *Pseudomonas* evades immune recognition of flagellin in both mammals and plants. PLoS Pathog. **7:** e1002206.

Beck, M., Zhou, J., Faulkner, C., MacLean, D., and Robatzek, S. (2012). Spatio-temporal cellular dynamics of the *Arabidopsis* flagellin receptor reveal activation status-dependent endosomal sorting. Plant Cell **24:** 4205–4219.

Bowling, S.A., Guo, A., Cao, H., Gordon, A.S., Klessig, D.F., and Dong, X. (1994). A mutation in *Arabidopsis* that leads to constitutive expression of systemic acquired resistance. Plant Cell **6:** 1845–1857.

Chinchilla, D., Bauer, Z., Regenass, M., Boller, T., and Felix, G. (2006). The *Arabidopsis* receptor kinase FLS2 binds flg22 and determines the specificity of flagellin perception. Plant Cell **18:** 465–476.

Choi, S.-W., Tamaki, T., Ebine, K., Uemura, T., Ueda, T., and Nakano, A. (2013). RABA members act in distinct steps of subcellular trafficking of the FLAGELLIN SENSING2 receptor. Plant Cell **25:** 1174–1187.

Christoforidis, S., McBride, H.M., Burgoyne, R.D., and Zerial, M. (1999a). The Rab5 effector EEA1 is a core component of endosome docking. Nature **397:** 621–625.

Christoforidis, S., Miaczynska, M., Ashman, K., Wilm, M., Zhao, L., Yip, S.-C., Waterfield, M.D., Backer, J.M., and Zerial, M. (1999b). Phosphatidylinositol-3-OH kinases are Rab5 effectors. Nat. Cell Biol. **1:** 249–252.

Citovsky, V., Lee, L.-Y., Vyas, S., Glick, E., Chen, M.-H., Vainstein, A., Gafni, Y., Gelvin, S.B., and Tzfira, T. (2006). Subcellular localization of interacting proteins by bimolecular fluorescence complementation *in planta*. J. Mol. Biol. **362:** 1120–1131.

Clough, S.J., and Bent, A.F. (1998). Floral dip: A simplified method for *Agrobacterium*-mediated transformation of *Arabidopsis thaliana*. Plant J. **16:** 735–743.

Coates, J.C. (2003). Armadillo repeat proteins: Beyond the animal kingdom. Trends Cell Biol. **13:** 463–471.

DebRoy, S., Thilmony, R., Kwack, Y.B., Nomura, K., and He, S.Y. (2004). A family of conserved bacterial effectors inhibits salicylic acid-mediated basal immunity and promotes disease necrosis in plants. Proc. Natl. Acad. Sci. USA **101:** 9927–9932.

De Camilli, P., Chen, H., Hyman, J., Panepucci, E., Bateman, A., and Brunger, A.T. (2002). The ENTH domain. FEBS Lett. **513:** 11–18.

Ellinger, D., Glöckner, A., Koch, J., Naumann, M., Stürtz, V., Schütt, K., Manisseri, C., Somerville, S.C., and Voigt, C.A. (2014). Interaction of the Arabidopsis GTPase RabA4c with its effector PMR4 results in complete penetration resistance to powdery mildew. Plant Cell **26:** 3185–3200.

Feraru, E., Feraru, M.I., Asaoka, R., Paciorek, T., De Rycke, R., Tanaka, H., Nakano, A., and Friml, J. (2012). BEX5/RabA1b regulates trans-Golgi network-to-plasma membrane protein trafficking in *Arabidopsis*. Plant Cell **24:** 3074–3086.

Furt, F., König, S., Bessoule, J.-J., Sargueil, F., Zallot, R., Stanislas, T., Noirot, E., Lherminier, J., Simon-Plas, F., Heilmann, I., and Mongrand, S. (2010). Polyphosphoinositides are enriched in plant membrane rafts and form microdomains in the plasma membrane. Plant Physiol. **152:** 2173–2187.

Geldner, N., Dénervaud-Tendon, V., Hyman, D.L., Mayer, U., Stierhof, Y.-D., and Chory, J. (2009). Rapid, combinatorial analysis of membrane compartments in intact plants with a multicolor marker set. Plant J. **59:** 169–178.

Gietz, R.D., and Woods, R.A. (1994). High efficiency transformation with lithium acetate in yeast. In Molecular Genetics of Yeast: A Practical Approach, J.R. Johnston, ed (Oxford, UK: IRL Press), pp. 121–134.

Godi, A., Di Campli, A., Konstantakopoulos, A., Di Tullio, G., Alessi, D.R., Kular, G.S., Daniele, T., Marra, P., Lucocq, J.M., and De Matteis, M.A. (2004). FAPPs control Golgi-to-cell-surface membrane traffic by binding to ARF and PtdIns(4)P. Nat. Cell Biol. **6:** 393–404.

Göhre, V., Spallek, T., Häweker, H., Mersmann, S., Mentzel, T., Boller, T., de Torres, M., Mansfield, J.W., and Robatzek, S. (2008). Plant pattern-recognition receptor FLS2 is directed for degradation by the bacterial ubiquitin ligase AvrPtoB. Curr. Biol. **18:** 1824–1832.

Gomez-Gomez, L., and Boller, T. (2000). FLS2: a LRR receptor-like kinase involved in recognition of the flagellin elicitor in Arabidopsis. Mol. Cell **5:** 1–20.

Gómez-Gómez, L., Bauer, Z., and Boller, T. (2001). Both the extracellular leucine-rich repeat domain and the kinase activity of FSL2 are required for flagellin binding and signaling in *Arabidopsis*. Plant Cell **13:** 1155–1163.

González-Lamothe, R., Tsitsigiannis, D.I., Ludwig, A.A., Panicot, M., Shirasu, K., and Jones, J.D.G. (2006). The U-box protein CMPG1 is required for efficient activation of defense mechanisms triggered by multiple resistance genes in tobacco and tomato. Plant Cell **18:** 1067–1083.

Grosshans, B.L., Ortiz, D., and Novick, P. (2006). Rabs and their effectors: Achieving specificity in membrane traffic. Proc. Natl. Acad. Sci. USA **103:** 11821–11827.

Gu, Y., Fu, Y., Dowd, P., Li, S., Vernoud, V., Gilroy, S., and Yang, Z. (2005). A Rho family GTPase controls actin dynamics and tip growth via two counteracting downstream pathways in pollen tubes. J. Cell Biol. **169:** 127–138.

Haas, T.J., Sliwinski, M.K., Martínez, D.E., Preuss, M., Ebine, K., Ueda, T., Nielsen, E., Odorizzi, G., and Otegui, M.S. (2007). The *Arabidopsis* AAA ATPase SKD1 is involved in multivesicular endosome function and interacts with its positive regulator LYST-INTERACTING PROTEIN5. Plant Cell **19:** 1295–1312.

Hatakeyama, S., Yada, M., Matsumoto, M., Ishida, N., and Nakayama, K.-I. (2001). U box proteins as a new family of ubiquitin-protein ligases. J. Biol. Chem. **276:** 33111–33120.

Hu, C.-D., Chinenov, Y., and Kerppola, T.K. (2002). Visualization of interactions among bZIP and Rel family proteins in living cells using bimolecular fluorescence complementation. Mol. Cell **9:** 789–798.

Hutagalung, A.H., and Novick, P.J. (2011). Role of Rab GTPases in membrane traffic and cell physiology. Physiol. Rev. **91:** 119–149.

Hyman, J., Chen, H., Di Fiore, P.P., De Camilli, P., and Brunger, A.T. (2000). Epsin 1 undergoes nucleocytosolic shuttling and its eps15 interactor NH_2-terminal homology (ENTH) domain, structurally similar to *Armadillo* and HEAT repeats, interacts with the transcription factor promyelocytic leukemia Zn^{2+} finger protein (PLZF). J. Cell Biol. **149:** 537–546.

Ishiga, Y., Ishiga, T., Uppalapati, S.R., and Mysore, K.S. (2011). *Arabidopsis* seedling flood-inoculation technique: A rapid and reliable assay for studying plant-bacterial interactions. Plant Methods **7:** 32.

Itoh, T., Koshiba, S., Kigawa, T., Kikuchi, A., Yokoyama, S., and Takenawa, T. (2001). Role of the ENTH domain in phosphatidylinositol-4,5-bisphosphate binding and endocytosis. Science **291:** 1047–1051.

Kang, B.-H., Nielsen, E., Preuss, M.L., Mastronarde, D., and Staehelin, L.A. (2011). Electron tomography of RabA4b- and PI-4Kβ1-labeled trans Golgi network compartments in *Arabidopsis*. Traffic **12:** 313–329.

Korasick, D.A., McMichael, C., Walker, K.A., Anderson, J.C., Bednarek, S.Y., and Heese, A. (2010). Novel functions of *Stomatal Cytokinesis-Defective 1* (*SCD1*) in innate immune responses against bacteria. J. Biol. Chem. **285:** 23342–23350.

Lee, Y., Kim, Y.-W., Jeon, B.W., Park, K.-Y., Suh, S.J., Seo, J., Kwak, J.M., Martinoia, E., Hwang, I., and Lee, Y. (2007). Phosphatidylinositol

4,5-bisphosphate is important for stomatal opening. Plant J. **52:** 803–816.

Li, W., et al. (2012a). The U-box/ARM E3 ligase PUB13 regulates cell death, defense, and flowering time in Arabidopsis. Plant Physiol. **159:** 239–250.

Li, W., Dai, L., and Wang, G.-L. (2012b). PUB13, a U-box/ARM E3 ligase, regulates plant defense, cell death, and flowering time. Plant Signal. Behav. **7:** 898–900.

Li, X., Rivas, M.P., Fang, M., Marchena, J., Mehrotra, B., Chaudhary, A., Feng, L., Prestwich, G.D., and Bankaitis, V.A. (2002). Analysis of oxysterol binding protein homologue Kes1p function in regulation of Sec14p-dependent protein transport from the yeast Golgi complex. J. Cell Biol. **157:** 63–77.

Liew, F.Y., Xu, D., Brint, E.K., and O'Neill, L.A.J. (2005). Negative regulation of toll-like receptor-mediated immune responses. Nat. Rev. Immunol. **5:** 446–458.

Liu, J., Li, W., Ning, Y., Shirsekar, G., Cai, Y., Wang, X., Dai, L., Wang, Z., Liu, W., and Wang, G.-L. (2012). The U-box E3 ligase SPL11/PUB13 is a convergence point of defense and flowering signaling in plants. Plant Physiol. **160:** 28–37.

Lu, D., Lin, W., Gao, X., Wu, S., Cheng, C., Avila, J., Heese, A., Devarenne, T.P., He, P., and Shan, L. (2011). Direct ubiquitination of pattern recognition receptor FLS2 attenuates plant innate immunity. Science **332:** 1439–1442.

Mudgil, Y., Shiu, S.-H., Stone, S.L., Salt, J.N., and Goring, D.R. (2004). A large complement of the predicted Arabidopsis ARM repeat proteins are members of the U-box E3 ubiquitin ligase family. Plant Physiol. **134:** 59–66.

Mueller-Roeber, B., and Pical, C. (2002). Inositol phospholipid metabolism in Arabidopsis: Characterized and putative isoforms of inositol phospholipid kinase and phosphoinositide-specific phospholipase C. Plant Physiol. **130:** 22–46.

Nielsen, E., Christoforidis, S., Uttenweiler-Joseph, S., Miaczynska, M., Dewitte, F., Wilm, M., Hoflack, B., and Zerial, M. (2000). Rabenosyn-5, a novel Rab5 effector, is complexed with hVPS45 and recruited to endosomes through a FYVE finger domain. J. Cell Biol. **151:** 601–612.

Nishimura, M.T., Stein, M., Hou, B.-H., Vogel, J.P., Edwards, H., and Somerville, S.C. (2003). Loss of a callose synthase results in salicylic acid-dependent disease resistance. Science **301:** 969–972.

Ohi, M.D., Vander Kooi, C.W., Rosenberg, J.A., Chazin, W.J., and Gould, K.L. (2003). Structural insights into the U-box, a domain associated with multi-ubiquitination. Nat. Struct. Biol. **10:** 250–255.

Pereira-Leal, J.B., and Seabra, M.C. (2001). Evolution of the Rab family of small GTP-binding proteins. J. Mol. Biol. **313:** 889–901.

Preuss, M.L., Schmitz, A.J., Thole, J.M., Bonner, H.K.S., Otegui, M.S., and Nielsen, E. (2006). A role for the RabA4b effector protein PI-4Kbeta1 in polarized expansion of root hair cells in *Arabidopsis thaliana*. J. Cell Biol. **172:** 991–998.

Preuss, M.L., Serna, J., Falbel, T.G., Bednarek, S.Y., and Nielsen, E. (2004). The Arabidopsis Rab GTPase RabA4b localizes to the tips of growing root hair cells. Plant Cell **16:** 1589–1603.

Raab, S., Drechsel, G., Zarepour, M., Hartung, W., Koshiba, T., Bittner, F., and Hoth, S. (2009). Identification of a novel E3 ubiquitin ligase that is required for suppression of premature senescence in Arabidopsis. Plant J. **59:** 39–51.

Robatzek, S., Chinchilla, D., and Boller, T. (2006). Ligand-induced endocytosis of the pattern recognition receptor FLS2 in *Arabidopsis*. Genes Dev. **20:** 537–542.

Robinson, D.G., Jiang, L., and Schumacher, K. (2008). The endosomal system of plants: Charting new and familiar territories. Plant Physiol. **147:** 1482–1492.

Salomon, S., and Robatzek, S. (2006). Induced endocytosis of the receptor kinase FLS2. Plant Signal. Behav. **1:** 293–295.

Samuel, M.A., Chong, Y.T., Haasen, K.E., Aldea-Brydges, M.G., Stone, S.L., and Goring, D.R. (2009). Cellular pathways regulating responses to compatible and self-incompatible pollen in *Brassica* and *Arabidopsis* stigmas intersect at Exo70A1, a putative component of the exocyst complex. Plant Cell **21:** 2655–2671.

Samuel, M.A., Mudgil, Y., Salt, J.N., Delmas, F., Ramachandran, S., Chilelli, A., and Goring, D.R. (2008). Interactions between the S-domain receptor kinases and AtPUB-ARM E3 ubiquitin ligases suggest a conserved signaling pathway in Arabidopsis. Plant Physiol. **147:** 2084–2095.

Schnatwinkel, C., Christoforidis, S., Lindsay, M.R., Uttenweiler-Joseph, S., Wilm, M., Parton, R.G., and Zerial, M. (2004). The Rab5 effector Rabankyrin-5 regulates and coordinates different endocytic mechanisms. PLoS Biol. **2:** E261.

Simonsen, A., Lippé, R., Christoforidis, S., Gaullier, J.-M., Brech, A., Callaghan, J., Toh, B.H., Murphy, C., Zerial, M., and Stenmark, H. (1998). EEA1 links PI(3)K function to Rab5 regulation of endosome fusion. Nature **394:** 494–498.

Sparkes, I.A., Runions, J., Kearns, A., and Hawes, C. (2006). Rapid, transient expression of fluorescent fusion proteins in tobacco plants and generation of stably transformed plants. Nat. Protoc. **1:** 2019–2025.

Stenmark, H. (2009). Rab GTPases as coordinators of vesicle traffic. Nat. Rev. Mol. Cell Biol. **10:** 513–525.

Stenmark, H., Parton, R.G., Steele-Mortimer, O., Lütcke, A., Gruenberg, J., and Zerial, M. (1994). Inhibition of rab5 GTPase activity stimulates membrane fusion in endocytosis. EMBO J. **13:** 1287–1296.

Stone, S.L., Anderson, E.M., Mullen, R.T., and Goring, D.R. (2003). ARC1 is an E3 ubiquitin ligase and promotes the ubiquitination of proteins during the rejection of self-incompatible *Brassica* pollen. Plant Cell **15:** 885–898.

Strahl, T., Hama, H., DeWald, D.B., and Thorner, J. (2005). Yeast phosphatidylinositol 4-kinase, Pik1, has essential roles at the Golgi and in the nucleus. J. Cell Biol. **171:** 967–979.

Szumlanski, A.L., and Nielsen, E. (2009). The Rab GTPase RabA4d regulates pollen tube tip growth in *Arabidopsis thaliana*. Plant Cell **21:** 526–544.

Thole, J.M., and Nielsen, E. (2008). Phosphoinositides in plants: Novel functions in membrane trafficking. Curr. Opin. Plant Biol. **11:** 620–631.

Trujillo, M., Ichimura, K., Casais, C., and Shirasu, K. (2008). Negative regulation of PAMP-triggered immunity by an E3 ubiquitin ligase triplet in *Arabidopsis*. Curr. Biol. **18:** 1396–1401.

Ueda, T., Yamaguchi, M., Uchimiya, H., and Nakano, A. (2001). Ara6, a plant-unique novel type Rab GTPase, functions in the endocytic pathway of *Arabidopsis thaliana*. EMBO J. **20:** 4730–4741.

Uknes, S., Mauch-Mani, B., Moyer, M., Potter, S., Williams, S., Dincher, S., Chandler, D., Slusarenko, A., Ward, E., and Ryals, J. (1992). Acquired resistance in *Arabidopsis*. Plant Cell **4:** 645–656.

van Loon, L.C., and van Strien, E.A. (1999). The families of pathogenesis-related proteins, their activities, and comparative analysis of PR-1 type proteins. Physiol. Mol. Plant Pathol. **554:** 85–97.

van Loon, L.C., Pierpont, W.S., Boller, T., and Conejero, V. (1994). Recommendations for naming plant pathogenesis-related proteins. Plant Mol. Biol. Rep. **12:** 245–264.

van Loon, L.C., Rep, M., and Pieterse, C.M.J. (2006). Significance of inducible defense-related proteins in infected plants. Annu. Rev. Phytopathol. **44:** 135–162.

Vega-Sánchez, M.E., Zeng, L., Chen, S., Leung, H., and Wang, G.-L. (2008). SPIN1, a K homology domain protein negatively regulated and ubiquitinated by the E3 ubiquitin ligase SPL11, is involved in flowering time control in rice. Plant Cell **20:** 1456–1469.

Vernoud, V., Horton, A.C., Yang, Z., and Nielsen, E. (2003). Analysis of the small GTPase gene superfamily of Arabidopsis. Plant Physiol. **131:** 1191–1208.

Voigt, B., et al. (2005). Actin-based motility of endosomes is linked to the polar tip growth of root hairs. Eur. J. Cell Biol. **84:** 609–621.

Vorwerk, S., Schiff, C., Santamaria, M., Koh, S., Nishimura, M., Vogel, J., Somerville, C., and Somerville, S. (2007). EDR2 negatively regulates salicylic acid-based defenses and cell death during powdery mildew infections of Arabidopsis thaliana. BMC Plant Biol. **7:** 35.

Walch-Solimena, C., and Novick, P. (1999). The yeast phosphatidylinositol-4-OH kinase pik1 regulates secretion at the Golgi. Nat. Cell Biol. **1:** 523–525.

Walsh, B.W., Lenhart, J.S., Schroeder, J.W., and Simmons, L.A. (2012). Far western blotting as a rapid and efficient method for detecting interactions between DNA replication and DNA repair proteins. Methods Mol. Biol. **922:** 161–168.

Wang, Y.J., Wang, J., Sun, H.Q., Martinez, M., Sun, Y.X., Macia, E., Kirchhausen, T., Albanesi, J.P., Roth, M.G., and Yin, H.L. (2003). Phosphatidylinositol 4 phosphate regulates targeting of clathrin adaptor AP-1 complexes to the Golgi. Cell **114:** 299–310.

Yan, J., Wang, J., Li, Q., Hwang, J.R., Patterson, C., and Zhang, H. (2003). AtCHIP, a U-box-containing E3 ubiquitin ligase, plays a critical role in temperature stress tolerance in Arabidopsis. Plant Physiol. **132:** 861–869.

Yang, C.-W., González-Lamothe, R., Ewan, R.A., Rowland, O., Yoshioka, H., Shenton, M., Ye, H., O'Donnell, E., Jones, J.D.G., and Sadanandom, A. (2006). The E3 ubiquitin ligase activity of *Arabidopsis* PLANT U-BOX17 and its functional tobacco homolog ACRE276 are required for cell death and defense. Plant Cell **18:** 1084–1098.

Zeng, L.-R., Qu, S., Bordeos, A., Yang, C., Baraoidan, M., Yan, H., Xie, Q., Nahm, B.H., Leung, H., and Wang, G.-L. (2004). *Spotted leaf11*, a negative regulator of plant cell death and defense, encodes a U-box/armadillo repeat protein endowed with E3 ubiquitin ligase activity. Plant Cell **16:** 2795–2808.

Zerial, M., and McBride, H. (2001). Rab proteins as membrane organizers. Nat. Rev. Mol. Cell Biol. **2:** 107–117.